Analysis of Weighted ℓ_1-minimization for Model Based Compressed Sensing.

by

Sidhant Misra

B.Tech., Electrical Engineering
Indian Institute of Technology, Kanpur (2008)

Submitted to the Department of Electrical Engineering and Computer Science
in partial fulfillment of the requirements for the degree of

Master of Science

at the

MASSACHUSETTS INSTITUTE OF TECHNOLOGY

February 2011

Author .....
Department of Electrical Engineering and Computer Science
January 21, 2011

Certified by .....
Pablo A. Parrilo
Professor
Thesis Supervisor

Accepted by .....
Terry P. Orlando
Chairman, Department Committee on Graduate Theses

Analysis of Weighted ℓ_1-minimization for Model Based Compressed Sensing.

by

Sidhant Misra

Submitted to the Department of Electrical Engineering and Computer Science
on January 21, 2011, in partial fulfillment of the
requirements for the degree of
Master of Science

Abstract

The central problem of Compressed Sensing is to recover a sparse signal from fewer measurements than its ambient dimension. Recent results by Donoho, and Candès and Tao giving theoretical guarantees that ℓ_1-minimization succeeds in recovering the signal in a large number of cases have stirred up much interest in this topic. Subsequent results followed, where prior information was imposed on the sparse signal and algorithms were proposed and analyzed to incorporate this prior information. In[13] Xu suggested the use of weighted ℓ_1-minimization in the case where the additional prior information is probabilistic in nature for a relatively simple probabilistic model.

In this thesis, we exploit the techniques developed in [13] to extend the analysis to a more general class of probabilistic models, where the probabilities are evaluations of a continuous function at uniformly spaced points in a given interval. For this case, we use weights which have a similar characterization . We demonstrate our techniques through numerical computations for a certain class of weights and compare some of our results with empirical data obtained through simulations.

Thesis Supervisor: Pablo A. Parrilo
Title: Professor

Acknowledgments

I would like to thank my advisor Pablo Parrilo for guiding me through my research. Through the numerous discussions we had, he gave me great insights and helped me learn several mathematical ideas and techniques.

I would like to thank my colleagues in LIDS for making the environment inspiring and enjoyable. I thank Parikshit Shah, Michael Rinehart and Mesrob Ohannessian for their useful advise and encouragement.

I am greatly thankful to Aliaa for her infinite support during the whole course of my masters. To my parents, I can never be thankful enough. Their unconditional love and encouragement has always been my guiding force.

Contents

1 Introduction **11**

1.1 Compressed Sensing 11

1.2 Model-Based Compressed Sensing 13

1.3 Organization of the thesis and Contribution 15

2 Background and previous work **17**

2.1 The ℓ_1-minimization method 17

2.1.1 Restricted Isometry Property 18

2.1.2 Neighborliness of Randomly Projected Polytopes. 20

2.2 Iterative Recovery Methods 23

2.3 Model Based Compressed Sensing 25

2.3.1 Deterministic model 25

2.3.2 Probabilistic model 28

3 Weighted ℓ_1-minimization for a specific family of weights- Formulation and Analysis **31**

3.1 Derivation of Internal and External Angles 32

3.1.1 Internal Angle 33

3.1.2 External Angle 36

3.2 Angle Exponents for a specific class of weights 37
3.2.1 Internal Angle Exponent 38
3.2.2 External Angle Exponent 41
3.3 Derivation of the critical Threshold 43
3.4 Improving the Bound on the Exponents 46
3.4.1 Combinatorial Exponent 48
3.4.2 External Angle Exponent 48
3.4.3 Internal Angle Exponent 49
3.5 Concavity of the Exponent Functions 51
3.6 Incorporating the probabilities in the derivation. 54
3.6.1 Bounding the probability of error and ϵ-typicality 55
3.6.2 Exponents 62

4 Numerical Computations and Simulations **65**
4.1 Behavior of F_0 under random projection. 66
4.2 Performance of weighted ℓ_1-minimization. 69

5 Conclusion and Future Work **73**

List of Figures

3-1 Maximum recoverable δ vs r computed using the methods of this section. 51

4-1 Lower bound on maximum recoverable δ vs ρ for the "first face" F_0, computed using the methods developed in Chapter 3 for $r = 30$ . . . 67

4-2 Empirical probability of error P_f vs δ with $\rho = 0$ for F_0 obtained through simulations using m = 200, n = 400 and 100 iterations. The vertical line refers to the lower bound computed using methods of Chapter 3. 68

4-3 Empirical probability of error P_f vs δ with $\rho = 1$ for F_0 obtained through simulations using m = 200, n = 400 and 100 iterations. The vertical line refers to the lower bound computed using methods of Chapter 3. 68

4-4 Lower bound on recoverable δ vs ρ for $\frac{m}{n} = 0.5$ computed using the methods of Chapter 3, for $c = 0.26$ and $c = 0.36$. The parameter r is fixed at 30. 70

4-5 Lower bound on recoverable δ vs ρ for $\frac{m}{n} = 0.5$ computed using the methods of Chapter 3, for $c = 0.26$ and $c = 0.36$. The parameter r is fixed at 60. 71

4-6 Empirical probability of error P_f vs c. Probability function $p(u) = 0.185 - c(u - 0.5)$. Problem size is given by $m = 500$, $n = 1000$. Number of iterations = 500. 72

Chapter 1

Introduction

1.1 Compressed Sensing

Compressed Sensing refers to obtaining linear measurements of a signal and compressing simultaneously and has been an area of much interest recently. Previously, the most common way to view recovery of signals from its samples was based on the Nyquist criterion. According to the Nyquist criterion for band-limited signals, the signals have to be sampled at twice the bandwidth to allow exact recovery. This is true for general band-limited signals but does not take into account any additional structure of the signal that might be known. In compressed sensing literature, the additional structure considered is that the signal is sparse with respect to a certain known basis. As opposed to sampling at Nyquist rate and subsequently compressing, measurements are now obtained by the action of linear operators on the signal. After fixing the basis with respect to which the signal is sparse, the process of obtaining the measurements can be written as $y = Ax$, where, $y \in \mathbb{R}^m$ is the vector of measurements, $x \in \mathbb{R}^n$ is the signal and $A \in \mathbb{R}^{m \times n}$ represents the m linear func-

tionals acting on the signal x. The signal x is considered to have at most k non-zero components. Compressed Sensing revolves around the fact that for sparse signals, the number of such linear measurements needed to reconstruct the signal can be significantly smaller than the ambient dimension of the signal itself. This recovery method aims at finding the sparsest solution x satisfying the constraints imposed by the measurements y which we represent by,

$$\begin{aligned} \min \quad & ||x||_0 \\ \text{subject to} \quad & y = Ax. \end{aligned}$$

Note that this problem is inherently combinatorial in nature. For a certain value of the size of the support given by k, it involves searching through all possible $\binom{n}{k}$ possible supports of the signal resulting in a NP-hard problem. Seminal work by Candés and Tao in [5] and Donoho in [7] show that under certain conditions on the linear operator in consideration, ℓ_1 norm minimization, which can be recast as a linear program, can recover the signal from its measurements. The implication of this result is profound. Linear programming is known to have polynomial time complexity, and the above mentioned result tells us that for a large class of problems we can solve an otherwise combinatorial problem in polynomial time. Subsequently, iterative methods based on a greedy approach were formulated which recover the signal from its measurements by obtaining an increasingly accurate approximation to the actual signal in each iteration. Examples of these include CoSaMP [10] and IHT [3]. In Chapter 2, we will give a fairly detailed description of CoSaMP and its performance.

1.2 Model-Based Compressed Sensing

Most of the earlier literature on Compressed Sensing focused on the case where the only constraints on the signal x are those imposed by its measurements y. On the other hand it is natural to consider the case where apart from sparsity, there is certain additional information on the structure of the underlying signal known to us. It would still of course be a valid approach to use some of the previously suggested methods such as ℓ_1-minimization or CoSamp, but this would fail to exploit this additional information. It would be of interest to devise recovery methods specific to the case at hand. Furthermore, one would also want to know if using the new recovery method gives us benefits over the previous method (lesser number of required measurements for the same level of sparsity of the signal). The authors in [2] introduced a deterministic signal model. The support of the underlying signal under this model is constrained to belong to a given known set. This defines a subset $\mathcal{M}$ of the set of all k-sparse signals, which is now the set of allowable signals. This results in an additional constraint on the original problem.

$$\begin{aligned} \min \quad & ||x||_0 \\ \text{subject to} \quad & y = Ax, \\ & x \in \mathcal{M}. \end{aligned}$$

It turns out that a simple modification to the CoSamp or IHT actually succeeds in exploiting the information about the model. The key property defined in [5], known as the Restricted Isometry Property was adapted in [2] to a a model based setting. With this, it was shown that results similar to [5] can be obtained for the model-based signal recovery. The fact that the number of sparse signals in the model $\mathcal{M}$

is now fewer than the unconstrained case allows us to use lesser number of linear measurements.

As opposed to this, Xu in [13] considers a probabilistic model. Under this model there are certain known probabilities associated with the components of the signal x. Specifically, $p_i, i = 1, 2, \ldots, n$ with $0 \leq p_i \leq 1$ are such that

$$\mathbf{P}(x_i \text{ is non-zero}) = p_i \qquad i = 1, 2, \ldots, n.$$

Use of a weighted ℓ_1-minimization as opposed to the standard ℓ_1-minimization was suggested for this case. This can be written as

$$\begin{aligned} \min \quad & ||x||_{w,1} \\ \text{subject to} \quad & y = Ax, \end{aligned}$$

where $||x||_{w,1} = \sum_{i=1}^{n} w_i|x_i|$ denotes the weighted ℓ_1 norm of x for a certain set of positive scalars $w_i, i = 1, , 2, \ldots, n$. High dimensional geometry based ideas similar to those in [7] were used to provide sufficient conditions under which this linear program recovers the sparse signal. The specific model considered involves a partition of the indices 1 to n into two disjoint sets T_1 and T_2. The probabilities described above are given by $p_i = P_1, i \in T_1$ and $p_i = P_2, i \in T_2$. Naturally, the weights used are $w_i = W_1, i \in T_1$ and $w_i = W_1, i \in T_1$. We will give a more detailed discussion on this in the next chapter.

1.3 Organization of the thesis and Contribution

In Chapter 2, we give a more comprehensive survey of the main results in Compressed Sensing literature, both for the standard and model-based case. Towards our contribution, in Chapter 3, we consider a more general probabilistic mode than in [13]. Consider a continuous monotonically decreasing function $p : [0, 1] \to [0, 1]$. Let the probability p_i that the i^{th} entry of x is non zero be given by

$$p_i = p\left(\frac{i}{n}\right).$$

The weighted l_1-minimization for recovering x from the measurements y is as follows:

$$\min \quad ||x||_{w,1}, \tag{1.1}$$

$$\text{subject to} \quad Ax = y. \tag{1.2}$$

For this case, we consider the positive weights w_i, which have a similar characterization

$$w_i = f\left(\frac{i}{n}\right),$$

where $f : [0, 1] \to \mathbb{R}$ is a continuous, positive and monotonically increasing function. The choice of a monotonically increasing $f(.)$ for a monotonically decreasing $p(.)$, is based on the intuition that we want to "encourage" the positions with higher prior probability to be more likely to be non-zero by assigning lower weights to them. We generalize the proof machinery in [13] to provide sufficient conditions for success of the weighted ℓ_1-minimization in our setting. In Chapter 4 we provide numerical and

simulation results, pointing out some of the salient features of our case. In Chapter 5, we conclude, with discussion on possible future works and interesting problems on this topic.

Chapter 2

Background and previous work

In this chapter we will describe some of the main results in Compressed Sensing. Most of the results show that under certain conditions on the parameters of the problem, computationally efficient methods such as ℓ_1-minimization succeeds in recovering the sparse signal from its measurements. It is difficult to prove such sufficient conditions for general deterministic matrices. So, typically in the literature it is assumed that the measurement matrix A is drawn from a random Gaussian ensemble, that is, the entries of the matrix are i.i.d Gaussian random variables with mean zero.

2.1 The ℓ_1-minimization method

In this section, we will present the seminal works of Candès and Tao [5] and Donoho [7] regarding the success of ℓ_1-minimization in recovering sparse signals from underdetermined systems. The approach in [5] is based on the so-called Restricted Isometry Property which is the topic of the following section. In the subsequent section, we will discuss the work in [7], based on the so-called neighborliness property of high

dimensional polytopes.

2.1.1 Restricted Isometry Property

Candès and Tao in [5] defined a notion of Restricted Isometry Property (RIP) for matrices. The RIP is in a sense a weaker notion of orthonormality and stems from the observation that in higher dimensions, two random vectors are nearly orthogonal to each other. In the subsequent parts $||x||$ will be used to refer to the ℓ_2 norm of the vector x.

Definition 2.1.1. [5] Let $A \in \mathbb{R}^{m \times n}$ be a matrix. For every integer $1 \leq k \leq n$, the k-Restricted Isometry constant δ_k is defined to be the smallest quantity such that for all vectors x with $|supp(x)| \leq k$, A satisfies

$$(1 - \delta_k)||x||^2 \leq ||Ax||^2 \leq (1 + \delta_k)||x||^2.$$

Similarly, the k_1, k_2 restricted orthogonality constant θ_{k_1,k_2} for $k_1 + k_2 \leq n$ is defined to be the smallest constant such that, for any vectors x_1, x_2 with disjoint supports which satisfy $|supp(x_1)| \leq k_1$ and $|supp(x_2)| \leq k_2$, A satisfies

$$|\langle Ax_1 Ax_2 \rangle| \leq \theta_{k_1,k_2}||x_1|| \cdot ||x_2||.$$

The constants δ_k and θ_{k_1,k_2} gives us an indication of how close the set of column vectors of A are to being an orthonormal system. Of course for an exact orthonormal system the vector x can be easily determined from its measurements $y = Ax$. However for sparse vectors, near-orthonormality in the sense of the RIP suffices. This is encapsulated in the following theorem.

Theorem 2.1.1. *[5] Assume that for a given k, with $1 \leq k \leq n$, the restricted isometry constants satisfy*

$$\delta_k + \theta_{k,k} + \theta_{k,2k} < 1.$$

Let $x \in \mathbb{R}^n$ be such that $|supp(x)| \leq k$, and let $y = Ax$. Then x is the unique solution of

$$\begin{aligned} \min \quad & ||x||_1 \\ \textit{subject to} \quad & Ax = y. \end{aligned}$$

While this theorem gives a sufficient condition for recovery, it is of interest to know when is this condition satisfied. Now, for a system to be strictly orthonormal, we must have $m = n$. Surprisingly, if the strictness is relaxed in the sense of the RIP, it is now possible to have a much larger number of column vectors and still satisfy the near orthonormality condition. Furthermore, matrices drawn from the random Gaussian ensemble with certain conditions on its dimensions satisfy this property with overwhelming probability.

Theorem 2.1.2. *[5] Let $A \in \mathbb{R}^{m \times n}$ with $m \leq n$ be a matrix with entries that are i.i.d Gaussian with mean 0 and variance $\frac{1}{m}$. Then there exists a constant $\delta^*(m,n)$ such that if $\frac{k}{n} = \delta$ satisfies $\delta \leq \delta^*(m,n)$, then the conditions on the Restricted Isometry Constants given in Theorem 2.1.1 are satisfied with overwhelming probability.*

It turns out that the constant $\delta^*(m,n)$ in the above theorem is such that for a given level of sparsity k, we need only $m = O(k \log(n/k))$ number of measurements to guarantee recovery, which is much smaller than the ambient dimension n.

The Restricted Isometry based analysis turned out to be a powerful tool in Compressed sensing and has been used extensively in subsequent work on the topic. Interestingly, it has been shown that recovery methods not based on ℓ_1-minimization can also guarantee recovery under certain conditions on the Restricted Isometry Constants.

2.1.2 Neighborliness of Randomly Projected Polytopes.

In this section we present an overview of the high dimensional geometry based approach introduced by Donoho to analyze the performance of ℓ_1-minimization. It revolves around the fact that the so-called neighborliness property of high dimensional polytopes has a strong connection to sparse solutions of underdetermined system of linear equations. Before proceeding, we provide a precise definition of this neighborliness property.

Definition 2.1.2. [6] A polytope P is called *k-neighborly* if every set of k vertices forms a $k-1$ dimensional face of the polytope. Similarly, a centrally symmetric polytope P is called *k-centrally-neighborly* if every set of k vertices not including antipodal pairs, form a $k-1$ dimensional face of P.

Consider the unit ℓ_1-ball C defined by

$$C = \{x \in \mathbb{R}^n | ||x||_1 \leq 1\}.$$

For a given measurement matrix A, one can talk of a corresponding quotient polytope $P = AC$ which is the image of C under the transformation defined by A. The theorem connecting neighborliness to recovery can then be stated as follows:

Theorem 2.1.3. *[6] The quotient polytope P of A is k-neighborly, if and only if*

for every $x_0 \in \mathbb{R}^n$ with at most k non-zero entries with $y = Ax_0$, x_0 is the unique solution to the optimization problem.

$$\begin{aligned} \min \quad & ||x||_1 \\ \textit{subject to} \quad & Ax = y. \end{aligned}$$

When $m < n$ and A has i.i.d. Gaussian entries, the polytope P can be interpreted as "a random projection" of the symmetric crosspolytope $C \subset \mathbb{R}^n$ onto a lower dimension m. One would expect that projecting onto a lower dimension would make the polytope "lose" faces. However it turns out that in higher dimensions, the lower dimensional faces "survive" with overwhelming probability. Therefore, it is of interest to characterize exact conditions under which this neighborliness holds. To this end, we need to define the face numbers of a polytope, $f_l(C)$ = the number of l-dimensional faces of polytope C. The polytope P is then *k-neighborly* if and only if $f_l(AC) = f_l(C), l = 0, 1, \ldots k-1$. We can now state the main Theorem in [7].

Theorem 2.1.4. *[7] Let $0 < \delta < 1$ be a constant. There exists a certain function $\rho_N : (0,1] \to [0,1]$, such that for $\rho < \rho_N(\delta)$, and a uniformly distributed random projection $A \in \mathbb{R}^{m \times n}$ with $m \geq \delta n$, we have*

$$\mathbf{P}\{f_l(AC) = f_l(C), \quad l = 0, 1, \ldots \rho m\} \to 1 \quad \textit{as } n \to \infty.$$

To prove this central theorem, the author makes use of powerful results in high dimensional geometry. Affentranger and Schneider in [1] proved the following result.

$$\mathbf{E}f_k(AC) = f_k(C) - 2\sum_{s \geq 0} \sum_{F \in J_k(C)} \sum_{G \in J_{m+1+2s}(C)} \beta(F,G)\gamma(G,C).$$

where $Ef_k(AC)$ refers to the expectation over all possible projections and $J_K(C)$ denotes the set of all $(k-1)$-dimensional faces of the polytope C. As there is a possibility that some of the $k-1$-dimensional faces of C are "swallowed" up by the projection, we always have $f_k(AC) \leq f_k(C)$. This in turn yields

$$\mathbf{P}\{f_k(AC) \neq f_k(C)\} \leq f_k(C) - \mathbf{E}f_k(AC) = 2\sum_{s\geq 0}\sum_{F\in J_k(C)}\sum_{G\in J_{m+1+2s}(C)} \beta(F,G)\gamma(G,C).$$

The quantity $\beta(F,G)$ is called the internal angle at face F of G and is the fraction of the unit hypershpere covered by the cone obtained by observing the face G from an internal point in F. For a given face G, $\gamma(G,C)$ is called the external angle of the polytope C at the face G and is defined as the fraction of the unit hypersphere covered by the cone formed by the outward normals to the supporting hyperplanes of C at the face G. In [7] the author then proceeds by showing that these internal and external angles decay exponentially with respect to n whenever $\rho \leq \rho_N(\delta)$.

The quantity $\rho_N(\delta)$ is called the *strong neighborliness threshold.* The "strong" refers to the fact that below the threshold, **all** the $k-1$-dimensional faces of C survive under the projection and the number $f_k(AC)$ is exactly equal to $f_k(C)$. This in turn guarantees that **all** k-sparse vectors x can be recovered by using ℓ_1-minimization. Corresponding to this, Vershik and Sporyshev in [12], study a weaker notion of threshold in the same setting. They derive a threshold corresponding to approximate equality of face numbers. Formally this can be written as follows.

Theorem 2.1.5. *Let $0 < \delta < 1$ be a constant. There exists a certain function $\rho_F : (0,1] \to [0,1]$, such that for $\rho < \rho_F(\delta)$, and a uniformly distributed random*

projection $A \in \mathbb{R}^{m \times n}$ *with* $m \geq \delta n$, *we have*

$$f_l(AC) = f_l(C) + o_P(1).$$

As will be described in the next section, this weak threshold is the one that will be useful when we consider probabilistic model based compressed sensing.

2.2 Iterative Recovery Methods

There have been some greedy-based algorithms that have been proposed to recover sparse signals from underdetermined systems. CoSamp[10] , and IHT[3] are among such methods with comprehensive theoretical guarantees. These algorithms proceed by constructing an approximation to the solution at each iteration. We will describe the CoSaMP algorithm in detail.

CoSaMP[10]

Initialization

$$a^0 = 0, v = y, i = 0.$$

Updating

$$i = i + 1$$

$$u = A^* v$$

$$\Omega = \text{supp}(u_{2k}), T = \text{supp}(a^{i-1}) \cup \Omega$$

$$b_T = A_T^+ y, b_{T^c} = 0$$

$$a^i = b_k$$

$$v = y - Aa^i.$$

Here, b_T is defined by $b_T(j) = b(T_j), 1 \leq j \leq |T|$, x_k, denotes the best *k-sparse* approximation in the least square sense to the vector x, and A_T^+ is the pseudo-inverse of the matrix A.

Note that if A were a perfectly orthonormal system, the step $u = A^* v$ would straight away give us back the vector x in the first iteration itself. Here, u serves as a "good" estimate for x because of the near-orthonormality of A in the sense of the RIP. Infact, the authors make use of an assumption on the restricted isometry constants to guarantee that this algorithm converges and recovers the correct x. We end this section with the main theorem from [10]

Theorem 2.2.1. *[10] Assume the matrix A satisfies $\delta_{4k} \leq 0.1$, then the estimation a^i at the end of the i^{th} iteration satisfies*

$$||x - a^i||_2 \leq 2^{-k}||x||_2 + 20\nu$$

Here ν refers to the so called unrecoverable energy which takes into account the noise in the measurements and imperfect sparsity of the vector x.

2.3 Model Based Compressed Sensing

In the previous two sections, we discussed about the basic compressed sensing problem and presented the two primary approaches to efficiently recover sparse solutions to underdetermined systems. In the basic problem, the constraints on the signal x are only those imposed by its measurements, i.e. $Ax = y$. It is then natural to consider the scenario when additional information about the signal is known a priori. The question arises as to what kind of prior information is of interest and how do we incorporate this prior information to our advantage. In the next couple of subsections, we will describe the two different kind of characterization of prior information that has been considered in recent literature and the corresponding suggested recovery methods and their performance.

2.3.1 Deterministic model

The authors in [2] considered the case when there is a deterministic model imposed on the support of the *k-sparse* vector x. Using the terminology of [2], we give the definition of this model. Let $x|_\Omega$ denote the entries of x corresponding to the set of indices $\Omega \subseteq \{1, 2, \ldots, n\}$.

Definition 2.3.1. [2] A signal model M_k is defined as the union of m_k canonical k-dimensional subspaces denoted by

$$M_k = \bigcup_{i-1}^{m_k} \chi_i \ , \chi_i = \{x : x|_{\Omega_i} \in \mathbb{R}^k, x|_{\Omega_i^C} = 0\}.$$

$\{\Omega_1, \ldots, \Omega_{m_k}\}$ are the set of possible supports that define this model.

To recover the x from its measurements based on this model, the authors proposed

a simple modification to the CoSamp and IHT algorithms. Before we present the modified CoSamp algorithm, we first give a couple of definitions from [2].

Definition 2.3.2. [2] For a positive integer B, the set M_k^B is defined as

$$M_k^B = \left\{ x : x = \sum_{r=1}^{B} x^r, x^r \in M_k. \right\}$$

Definition 2.3.3. [2] For a positive integer B, $M_B(x,k)$ is defined as

$$M_B(x,k) = \arg\min_{\bar{x} \in M_k^B} ||x - \bar{x}||^2.$$

which refers to the best model based Bk-sparse approximation to x.

The modification to the CoSamp Algorithm essentially involves replacing the best Bk-sparse approximations with the best model based Bk-sparse approximation. Surprisingly, this simple modification captures and exploits the information provided by the knowledge of the model very well.

Model Based CoSamp[2]

Initialization

$$a^0 = 0, v = y, i = 0.$$

Updating

$$i = i + 1$$

$$u = A^* v$$

$$\Omega = \text{supp}(M_2(u, k)), T = \text{supp}(a^{i-1}) \cup \Omega$$

$$b_T = A_T^+ y, b_{T^c} = 0$$

$$a^i = M_1(b, k)$$

$$v = y - Aa^i.$$

Of course for the algorithm to be efficient, finding best model based approximation to a given vector should allow efficient computation. The performance guarantees of the above algorithm provided in [2] are very similar to those in [10], except that it is now based on a model-based Restricted Isometry Property.

Definition 2.3.4. [2] *(Model Based RIP - M_k^B-RIP)* $A \in \mathbb{R}^{m \times n}$ is said to have the M_k^B restricted isometry property if there exists a constant $\delta_{M_k^B}$ such that for all $x \in M_k^B$, we have

$$(1 - \delta_{M_k^B})||x||^2 < ||Ax||^2 < (1 + \delta_{M_k^B})||x||^2.$$

We now state the theorem in [2] corresponding to Theorem 3.2.1, giving sufficient conditions on recovery for the model based CoSamp.

Theorem 2.3.1. *[2] Assume the matrix A satisfies $\delta_{M_k^4} \leq 0.1$, then the estimation a^i at the end of the i^{th} iteration satisfies*

$$||x - a^i||_2 \leq 2^{-k}||x||_2 + 20\nu$$

For a matrix A drawn from the random Gaussian ensemble to satisfy the model based RIP, we need $m = O(k + \log(m_k))$ [4]. For the unconstrained case (absence of any model), we have $m_k = \binom{n}{k}$ which gives $m = O(k \log(n/k))$ as before. This tells us that for more restrictive models (smaller m_k), we need much fewer measurements for recovering the signal if we use model based recovery methods (e.g. model based CoSAmp) as opposed to the standard methods for the unconstrained case.

2.3.2 Probabilistic model

In this subsection, we present in fair amount of detail the work by Xu in [13]. Our work is based on the methodology that we will discuss subsequently. We mention the main steps of this methodology so that our work, which is the content of the next chapter, will be in continuation of what we present in this subsection.

In [13], the author considered that there is a set of probabilities $p_1, \ldots, p_n$ known to us such that $\mathbf{P}\{x_i \neq 0\} = p_i$. The use of weighted ℓ_1-minimization is suggested to recover x from its measurements y and is given by,

$$\begin{aligned} \min \quad & \sum_{i=1}^{n} w_i |x_i| \\ \text{subject to} \quad & Ax = y. \end{aligned}$$

Intuitively, we would use a larger w_i corresponding to a smaller p_i. We are in some sense improving the chances of recovery for those sparse vectors with higher probability at the same time paying by reducing the chance of correct recovery for sparse vectors with low probability. By doing so we are aiming at enhancing the chances of recovery on an average. The notion of a strong threshold as described in the previous section is no longer applicable inthis case, because the strong threshold characterizes

the condition when *all* k-sparse x can be recovered. Also, the Restricted Isometry Property defined in section 2.1 treats all k-subset of columns of A uniformly and thus in its current form is not going to be useful in analyzing weighted ℓ_1-minimization. The author in [13] makes use of a method similar to the high dimensional geometry approach in [7], but considers the notion of weak threshold. Here,we give a detailed description of this notion.

Let P be the skewed crosspolytope given by $\{x \in \mathbb{R}^n \mid ||x||_{w,1} \leq 1\}$. Without loss of generality we can assume that the vector x has $||x||_{w,1} = 1$. Let the support set of x be given by $K = \{i_1, i_2, \ldots, i_k\}$. We fix a particular sign pattern for x, say all positive. Then x lies on the $k-1$ dimensional face F of the cross polytope P which is the convex hull of the vertices $e_{i_1}, \ldots, e_{i_k}$ where e_i denotes the vector in $\mathbb{R}^n$ with $\frac{1}{w_i}$ in the i^{th} position and 0 everywhere else. As any solution to the weighted ℓ_1-minimization problem satisfies $Ax = b$, the solution is of the form $x + u$ where u belongs to the null space of A. The event that an incorrect solution is obtained is precisely the event that there is a vector u in the null space of A such that $||x + u||_{w,1} < 1$. The following lemma regarding the null space of a matrix with i.i.d. Gaussian serves as a key observation.

Lemma 2.3.1. *Let $A \in \mathbb{R}^{m \times n}$ be a random matrix with i.i.d. $N(0,1)$ entries. Let Z be a matrix of column vectors spanning the null space of A. Then, the distribution of A is rotationally invariant and it is always possible to choose a basis such that the entries of Z are distributed independently according to a normal distribution with mean 0 and variance 1.*

This says that the null space of A is a random subspace and sampling from this null space is equivalent to uniformly sampling from the Grassman manifold $Gr_{(n-m)}(n)$. From the lemma and the preceding discussion, we can characterize the

probability of failure P_f, the probability that weigthed ℓ_1-minimization fails to recover the correct x. P_f is the probability that a uniformly chosen $n-m$ dimensional random subspace shifted to the point x on the face F intersects the crosspolytope P non trivially at some other point other than x. This is the so called complementary Grassmann Angle for the face F with respect to the polytope P under the Grassmann manifold $Gr_{(n-m)}(n)$. Based on work by Santalo [11] and McMullen [9] the Complementary Grassmann Angle can be can be expressed explicitly as the sum of products of internal and external angles as follows.

$$P_f = 2\sum_{s\geq 0}\sum_{G\in J(m+1+2s)} \beta(F,G)\gamma(G,P) \tag{2.1}$$

where $\beta(F,G)$ and $\gamma(G,P)$ are the internal and external angles defined previously. The author in [13] then proceeds by bounding the exponential rate of decay of the internal and external angles, to characterize the conditions under which the probability of failure P_f goes to zero with overwhelming probability. Much of this technique is suitably adapted to our case and will be presented in full detail in the next chapter.

Chapter 3

Weighted ℓ_1-minimization for a specific family of weights- Formulation and Analysis

In this chapter, we consider the problem of model based compressed sensing with a probabilistic model. Under this model, the probability that the i^{th} entry of the signal x is non-zero is given by

$$\mathbf{P}\{x_i \neq 0\} = p_i.$$

Specifically we consider the case when the probabilities p_i mentioned above are values of a continuous function at uniformly spaced points on a given interval. Let $p : [0,1] \to [0,1]$ be a continuous monotonically decreasing function. Then p_i is defined as $p_i = p\left(\frac{i}{n}\right)$. In this chapter, we will prove that under certain conditions similar to the threshold conditions in [13], for the class of weights under consideration, the probability that weighted ℓ_1-minimization fails to recover the correct sparse solution

will decay exponentially with respect to ambient dimension of the signal n. We also give bounds on the rate of this exponential decay, which will allow us to formulate conditions under which the the probability of failure of weighted ℓ_1-minimization to recover the correct x decays exponentially.

In section 3.1, we will derive the expressions for the Internal and External Angles described in section 2.3.2. In section 3.2, we will show that these internal and external angles can be bounded by exponential functions and obtain the corresponding exponents for these functions. Following this, in section 3.3, we will characterize the conditions under which the angles exponents decay exponentially. All of the above mentioned section focus on analyzing the behavior of a specific face of the skewed cross-polytope (see section 2.3.2). In sections 3.4 and 3.5 describe how we can enhance the accuracy of our bounds by exploiting the structure of the weights. In section 3.6, we generalize the machinery developed in the previous sections to give a bound on the probability of failure of weighted ℓ_1-minimization and characterize the conditions under which it decays exponentially with respect to n, the dimension of the signal x.

3.1 Derivation of Internal and External Angles

In this section we will derive the expressions for the internal and external angle defined by a specific pair of faces F and G of the unit weighted ℓ_1-ball P. The weights considered are denoted by $w_i, \quad i = 1, 2, \ldots, n$. We will maintain the generality of the weights in our discussion before specializing the expressions to our case in the next section. Let $1 < k < l < n$ be given. In the subsequent derivation, the face F_0 is the face corresponding to the corners given by $\frac{1}{w_1}e_1, \ldots, \frac{1}{w_k}e_k$, and G_0 is the face corresponding to the corners $\frac{1}{w_1}e_1, \ldots, \frac{1}{w_1}e_l$.

3.1.1 Internal Angle

We follow closely the method in [13]. We first outline the major steps in the derivation of $\beta(F_0, G_0)$.

1. The internal angle $\beta(F, G)$ is the fraction of the hypersphere S covered by the cone of feasible directions $Con_{F,G}$ for the face G at any interior point x_{F_0} of F_0. This is essentially the relative spherical volume of the cone Con_{F_0,G_0}.

2. Let L_{F_0} be the linear span $lin(F_0 - x_{F_0})$. Define $Con_{F_0 \perp G_0} = Con_{F_0,G} \cap {L_{F_0}}^{\perp}$, where ${L_{F_0}}^{\perp}$ denotes the orthogonal complement of L_{F_0}. Then the relative spherical volume of Con_{F_0,G_0} and $Con_{F_0 \perp G_0}$ are the same.

3. From [8], we have

$$\begin{aligned}
&\int_{Con_{F_0 \perp G_0}} exp(-||x||^2)dx \\
=&\beta(F_0, G_0)V_{l-k-1}(S^{l-k-1}) \times \int_0^{\infty} e^{-r^2} r^{l-k-1} dr \\
=&\beta(F_0, G_0)\pi^{\frac{(l-k)}{2}}.
\end{aligned}$$

For any internal point $x \in F_0$, define $Con_{F_0/G_0} = cone\{\frac{e_{k+1}}{w_{k+1}} - x, \ldots, \frac{e_l}{w_l} - x\}$. Then $Con_{F_0 \perp G_0} = Con_{F_0/G_0} \cap {L_{F_0}}^{\perp}$. Consider the point $\bar{x} \in F_0$ given by $\frac{1}{\sum_{i=1}^k w_i^2} \sum_{i=1}^k w_i^2 \times \frac{e_i}{w_i} = \frac{1}{\sum_{i=1}^k w_i^2} \sum_{i=1}^k w_i e_i$.

Note that every $y \in L_{F_0}$ satisfies

$$\sum_{i=1}^{k} w_i y_i = 0,$$

$$y_i = 0, \ i \geq k+1.$$

So for any $y_1 \in L_{F_0}$ and $y_2 \in Con_{F_0/G_0}$, we have $\langle y_1, y_2 \rangle = 0$ which means $Con_{F_0/G_0} \subset {L_{F_0}}^{\perp}$ and hence for this point $\bar{x}$, we have $Con_{F_0 \perp G_0} = Con_{F_0/G_0}$.

Any point in $Con_{F_0 \perp G_0}$ is now described by

$$\sum_{i=1}^{l-k} \alpha_i \left(\frac{e_{k+i}}{w_{k+i}} - \frac{1}{\sum_{j=1}^{k} w_j^2} \sum_{j=1}^{k} w_j e_j \right), \ \alpha_i \geq 0.$$

Now, we can easily transform this representation to the one given in [13]. Let $U \subseteq \mathbb{R}^{l-k+1}$ described by the set of all non-negative vectors x satisfying,

$$\left(\sum_{p=1}^{k} w_p^2 \right) x_1 = \sum_{p=k+1}^{l} w_p^2 x_{p-k+1}.$$

The following map describes every point in $Con_{F_0 \perp G_0}$ uniquely.

$$f_1(x_1, \ldots, x_{l-k+1}) = -\sum_{p=1}^{k} x_1 w_p e_p + \sum_{p=k+1}^{l} x_{p-k+1} w_p e_p.$$

The map $f_1 : U \to Con_{F_0 \perp G_0}$ is a bijective map. From here, we follow closely the steps outlined in [13]. The internal angle can then be computed as

$$\begin{aligned}\beta(F_0, G_0) &= \pi^{-\frac{l-k}{2}} \int_{Con_{F_0 \perp G_0}} e^{-||x||^2} dx \\ &= \int_U e^{-||f^2(x)||} df(x).\end{aligned}$$

We give the final expression.

$$\int_{Con_{F_0 \perp G_0}} e^{-||x||^2} dx = \rho_{k+1,l} \sqrt{\frac{\sigma_{1,l}}{\sigma_{1,k}}} \times$$
$$\int_{x_2,\ldots,x_{l-k+1} \geq 0} exp\{-x_1^2 \sigma_{1,k} - \sum_{p=k+1}^{l} x_{p-k+1}^2 w_p^2\} dx_2 \ldots dx_{l-k+1}.$$

where

$$\begin{aligned}x_1 &= \frac{1}{\sigma_{1,k}} \sum_{p=k+1}^{l} x_{p-k+1} w_p^2, \\ \sigma_{1,k} &= \sum_{i=1}^{k} w_i^2, \\ \rho_{p,q} &= \prod_{i=p}^{q} w_i.\end{aligned}$$

Let $Y_0 \sim N(0, \frac{1}{2})$ be a normal random variable and $Y_p \sim HN(0, \frac{w_{p+k}^2}{2\sigma_{1,k}})$ for $p = 1, 2, \ldots, l-k$ be half normal distributed random variables. Define the random variable $Z = Y_0 - \sum_{p=1}^{l-k} Y_p$. Then, by inspection we get

$$\beta(F_0, G_0) = \pi^{-\frac{l-k}{2}} \int_{Con_{F_0 \perp G_0}} e^{-||x||^2} dx = \frac{\sqrt{\pi}}{2^{l-k}} \sqrt{\frac{\sigma_{1,l}}{\sigma_{1,k}}} p_Z(0). \tag{3.1}$$

This gives us an expression for the internal angle of G_0 at face F_0 in terms of the weights w_i.

3.1.2 External Angle

We outline the method in [13], which we closely follow, for computing the external angle for the face G defined by the vertices $\frac{1}{w_1}e_1, \ldots, \frac{1}{w_l}e_l$.

1. The external angle $\gamma(G_0, P)$ is defined as the fraction of the hypersphere S covered by the cone of outward normals C_{G_0} to the hyperplanes supporting the cross polytope P and passing through the face G_0.

2. $\int_{C_{G_0}} exp(-||x||^2)dx = \gamma(G_0, P)\pi^{\frac{(n-l+1)}{2}}$.

3. Define the set $U \subseteq \mathbb{R}^{n-l+1}$ by

$$U = \{x \in \mathbb{R}^{n-l+1} | x_{n-l+1} \geq 0, |x_i/w_i| \leq x_{n-l+1}, 1 \leq i \leq n-l\}.$$

Let $f_2 : U \to c(G_0, C)$ be the bijective map defined by

$$f_2(x_1, \ldots, x_{n-l+1}) = \sum_{i=1}^{n-l} x_i e_i + \sum_{i=n-l+1}^{n} w_i x_{n-l+1} e_i.$$

Using this, we obtain the expression for the external angle as.

$$\gamma(G_0, C) = \pi^{\frac{-(n-l+1)}{2}} \int_{C_{G_0}} exp(-||x||^2)dx \qquad = \int_U e^{-||f^2(x)||} df(x).$$

After some algebra, we obtain the final expression for the external angle $\gamma(G_0, P)$

as

$$\gamma(G_0, P) = \pi^{-\frac{n-l+1}{2}} 2^{n-l} \int_0^\infty e^{-x^2} \prod_{p=l+1}^{n} (\int_0^{\frac{w_p x}{\sqrt{\sigma_{1,l}}}} e^{-y_p^2} dy_p) dx. \tag{3.2}$$

3.2 Angle Exponents for a specific class of weights

We aim at finding the asymptotic exponential behavior of the internal and external angles described in the previous section. Defining $\delta = \frac{k}{n}$ and $\gamma = \frac{l}{n}$ we aim at finding exponents $\psi_{int}(\delta, \gamma)$ and $\psi_{ext}(\gamma)$ for the internal and external angle respectively satisfying the following:

1. Given $\epsilon > 0$, δ, γ, $\exists n_0(\epsilon)$ such that for all $n > n_0(\epsilon)$
   $n^{-1} \log(\beta(F_0, G_0)) < \psi_{int}(\delta, \gamma) + \epsilon$.

2. Given $\epsilon > 0$, γ, $\exists n_0(\epsilon)$ such that for all $n > n_0(\epsilon)$
   $n^{-1} \log(\gamma(G_0, P)) < \psi_{ext}(\gamma) + \epsilon$.

What the above bounds will allow us to do is to formulate conditions on the parameters of the problem under which the image of the face F_0 in consideration, under the projection defined by A, will also be a face of the projected polytope (i.e. the face "survives" under the projection). In terms of sparse solutions to underdetermined systems, this translates to saying that if the signal x has its non-zero entries in the first k positions, then the weighted ℓ_1-minimization algorithm will successfully recover x from its measurements given by $y = Ax$. The derivation of the above exponents for a general set of weights w_i is rather computationally difficult. To demonstrate their methods the author in [13] derived the exponents for the case when the weights are chosen as $w_i = W_1$ for $1 \leq i \leq \lambda n$ and $w_i = W_2$ for $\lambda n < i \leq n$ where $0 < \lambda < 1$ is a fixed number. Here, we seek to derive the exponents when the

weights are "continuously" varying. Specifically, let $f : [0,1] \to \mathbb{R}^+$ be a continuous and monotonically increasing function. For a particular n, we choose the weights as $w_i = f(\frac{i}{n})$. We bound the internal and external angles corresponding to this choice of weights by exponential functions in n and characterize the exponents of these functions. This is the topic of the next two subsections.

3.2.1 Internal Angle Exponent

Recalling the expression for the internal angle

$$\beta(F,G) = \frac{1}{\sqrt{\pi}^{l-k}} \int_{Con_{F_0 \perp G_0}} e^{-\|x\|^2} dx = \frac{\sqrt{\pi}}{2^{l-k}} \sqrt{\frac{\sigma_{1,l}}{\sigma_{1,k}}} p_Z(0),$$

where $Z = -Y_0 + \sum_{p=1}^{l-k} Y_p$ with Y_i defined as before. Define $S = \sum_{p=1}^{l-k} Y_p$. $Z = Y_0 + S$. Using the convolution integral the density function of Z can be written as

$$\begin{aligned} p_Z(0) &= \int_{-\infty}^{\infty} p_{Y_0}(-v) p_S(v) dv \\ &= 2 \int_0^{\infty} v p_{Y_0}(v) F_S(v) dv, \end{aligned}$$

where $F_S(v)$ is the cumulative distribution function of S. Let μ_S be the mean of the random variable S. We get

$$p_Z(0) = \underbrace{2 \int_0^{\mu_S} v p_{Y_0}(v) F_S(v) dv}_{I} + \underbrace{2 \int_{\mu_S}^{\infty} v p_{Y_0}(v) F_S(v) dv}_{II}.$$

As in [7], the second term satisfies $II < e^{-\mu_S^2}$ and is negligible. For $v \leq \mu_S$, $F_S(v) \leq exp(-\lambda_S^*(v))$, where $\lambda_S^*(v)$ denotes the rate function (convex conjugate

of the characteristic function λ) of the random variable S. So we get

$$I \leq \frac{2}{\sqrt{\pi}} \int_0^{\mu_S} v e^{-v^2 - \lambda_S^*(v)} dv.$$

After a change in variables in the above integral, we get

$$I \leq \frac{2}{\sqrt{\pi}} \frac{s_{k+1,l}^2}{2\sigma_{1,k}} \int_0^{\sqrt{\frac{2}{\pi}}} y \exp[-\frac{s_{k+1,l}^2}{2\sigma_{1,k}} y^2 - s_{k+1,l} \lambda_0^*(y)] dy,$$

where

$$\lambda_0^*(y) = \max_s ys - \frac{1}{s_{k+1,l}} \sum_{p=1}^{l-k} \lambda(w_{p+k} s).$$

Now, as the weights w_i are the samples of the continuous function f, we have

$$s_{k+1,l} = \sum_{i=k+1}^{l} f\left(\frac{i}{n}\right) \sim n \int_\delta^\gamma f(x) dx.$$

Define $c_0(\delta, \gamma) = \int_\delta^\gamma f(x) dx$. This gives us $s_{k+1.l} = n c_0(\delta, \gamma)$. Similarly,

$$\sigma_{1,k} = \sum_{i=1}^{k} w_i^2 = \sum_{i=1}^{k} f^2\left(\frac{i}{n}\right) \sim n \int_0^\delta f^2(x) dx = n c_1(\delta),$$

where $c_1(\delta)$ is defined as $c_1(\delta) = \int_0^\delta f^2(x) dx$. This gives us

$$\begin{aligned} &\frac{s_{k+1.l}^2}{2\sigma_{k+1.l}} y^2 + s_{k+1,l} \lambda_0^*(y) \\ \approx &n \left(\frac{c_0^2}{2c_1} y^2 + c_0 \lambda^*(y) \right) = n\eta(y). \end{aligned}$$

where $\eta(y)$ is defined as $\eta(y) = \left(\frac{c_0^2}{2c_1}y^2 + c_0\lambda_0^*(y)\right)$. Using Laplace's method to bound the integral as in [7], we get

$$I \leq e^{-n\eta(y^*)}(R_n),$$

where $n^{-1}\log(R_n) = o(1)$, and y^* is the minimizer of the convex function $\eta(y)$. Let

$$\begin{aligned}\lambda_0^*(y^*) &= \max_s\, sy^* - \lambda_0(s) \\ &= s^*y^* - \lambda_0(s^*).\end{aligned}$$

Then the maximizing s^* satisfies $\lambda_0'(s^*) = y^*$. From convex duality, we have $\lambda_0^{*'}(y^*) = s^*$. The minimizing y^* of $\eta(y)$ is given by

$$\begin{aligned}&\frac{c_0^2}{c_1}y^* + c_0\lambda_0^{*'}(y^*) = 0 \\ \Longrightarrow\ &\frac{c_0^2}{c_1}y^* + c_0 s^* = 0. \end{aligned} \tag{3.3}$$

This gives

$$\lambda_0'(s^*) = -\frac{c_1}{c_0}s^*. \tag{3.4}$$

First we approximate $\lambda_0(s)$ as follows

$$\lambda_0(s) = \frac{1}{s_{k+1.l}}\sum_{p=1}^{l-k}\lambda(w_{p+k}s) \approx \frac{1}{nc_0}\sum_{p=k+1}^{l}\lambda\left(f\left(\frac{p}{n}\right)s\right) \approx \frac{1}{c_0}\int_\delta^\gamma \lambda\left(sf(x)\right)dx.$$

So,

$$\frac{d}{ds}\lambda_0(s) \approx \frac{d}{ds}\frac{1}{c_0}\int_\delta^\gamma \lambda\left(sf(x)\right)dx$$
$$= \frac{1}{c_0}\int_\delta^\gamma f(x)\lambda'\left(sf(x)\right)dx.$$

Combining this with equation 3.4, we can determine s^* by finding the solution to the equation

$$\int_\delta^\gamma f(x)\lambda'(s^*f(x))dx + c_1 s^* = 0. \tag{3.5}$$

Thus the internal angle exponent is given by

$$\psi_{int}(\beta,\gamma) = -\eta(y^*) = -\left(\frac{c_0^2}{2c_1}y^{*2} + c_0\lambda_0^*(y^*)\right), \tag{3.6}$$

where y^* is determined through s^* from equation 3.3 and s^* is determined by solving the equation 3.5.

3.2.2 External Angle Exponent

Recall the expression for the external angle

$$\gamma(G_0,P) = \pi^{-\frac{n-l+1}{2}}2^{n-l}\int_0^\infty e^{-x^2}\prod_{p=l+1}^{n}\left(\int_0^{\frac{w_p x}{\sqrt{\sigma_{1,l}}}} e^{-y_p^2}dy_p\right)dx.$$

The standard error function is by definition given by

$$\mathrm{erf}(x) = \frac{2}{\sqrt{\pi}} \int_0^x e^{-t^2} dt.$$

Using this we can rewrite

$$\gamma(G_0, P) = \sqrt{\frac{\sigma_{1,l}}{\pi}} \int_0^\infty e^{-\sigma_{1,l} x^2} \prod_{i=l+1}^{n} \mathrm{erf}(w_i x) dx.$$

Using a similar procedure to that used in the internal angle section

$$\sigma_{1,l} = \sum_{i=1}^{l} w_i^2 \sim n \int_0^\gamma f^2(x) dx = n c_2(\gamma).$$

where $c_2(\gamma)$ is defined as $c_2(\gamma) = \int_0^\gamma f^2(x) dx$. Substituting this we have

$$\begin{aligned} \gamma(G_0, P) &= \sqrt{\frac{\sigma_{1,l}}{\pi}} \int_0^\infty \exp\left[-n \left(c_2 x^2 - \frac{1}{n} \sum_{i=l+1}^{n} \log(\mathrm{erf}(w_i x)) \right) \right] dx \\ &= \sqrt{\frac{\sigma_{1,l}}{\pi}} \int_0^\infty \exp[-n\zeta(x)] dx. \end{aligned}$$

where $\zeta(x)$ is defined as $\zeta(x) = \left(c_2 x^2 - \frac{1}{n} \sum_{i=l+1}^{n} \log(\mathrm{erf}(w_i x)) \right)$. Again using Laplace's method we get

$$\gamma(G_0, P) \leq \exp[-n\zeta(x^*)] R_n,$$

where x^* is the minimizer of $\zeta(x)$ and $n^{-1}\log(R_n) = o(1)$ The minimizing x^* satisfies $2c_2x^* = G_0'(x^*)$, where

$$G_0(x) = \frac{1}{n}\sum_{i=l+1}^{n}\log(\mathrm{erf}(w_i x)).$$

We first approximate $G_0(x)$ as follows:

$$\begin{aligned} G_0(x) &= \frac{1}{n}\sum_{i=l+1}^{n}\log(\mathrm{erf}(w_i x)) \\ &= \frac{1}{n}\sum_{i=l+1}^{n}\log(\mathrm{erf}(f(i/n)x)) \approx \int_{\gamma}^{1}\log(\mathrm{erf}(xf(y)))dy. \end{aligned}$$

So the minimizing x^* can be computed by solving the equation

$$2c_2x^* = \int_{\gamma}^{1}\frac{f(y)\,\mathrm{erf}'(x(f(y))}{\mathrm{erf}(xf(y))}dy. \tag{3.7}$$

The external angle exponent of face G is therefore given by

$$\psi_{ext}(\gamma) = -\zeta(x^*) = -\left(c_2x^{*2} - \int_{\gamma}^{1}\log(\mathrm{erf}(x^*f(y)))dy\right). \tag{3.8}$$

and x^* can be obtained by solving equation 3.7.

3.3 Derivation of the critical Threshold

In the previous sections we established the fact that the internal and external angles can be bounded by exponential functions of n and derived the expressions for the exponents involved. We are now in a position to use this to formulate conditions under which the face F_0 survives the projection defined by A. In other words every vector

x which can be normalized to lie on the face F_0 can be successfully recovered through weighted ℓ_1-minimization with overwhelming probability. We do so by bounding the probability of failure of the weighted ℓ_1-minimization by an exponential function of n, and characterizing conditions which guarantee the exponent of this function to be negative. From our previous discussion, the probability of failure P_f is given by

$$P_f = 2 \sum_{s \geq 0} \sum_{G \in J(m+1+2s)} \beta(F, G)\gamma(G, P).$$

For a fixed value l, where G is a $l-1$ dimensional face of the polytope, the maximum value of $\beta(F, G)$ with G varying over all $l-1$ dimensional faces is attained by the face with the smallest set of indices as its corners. The same is also true for $\gamma(G, P)$. These facts can be easily seen from the expressions of the corresponding quantities and the fact that the weights w_i's are assumed to be monotonically increasing. This allows us to can upper bound the probability of error as

$$\begin{aligned} P_f &\leq \sum_{l=m+1}^{n} \binom{n-k}{l-k} 2^{l-k} \beta(F, G_1)\gamma(G_1, P) \\ &\leq (n-m) \max_l \{ \binom{n-k}{l-k} 2^{l-k} \beta(F, G_1)\gamma(G_1, P) \}, \end{aligned}$$

where G_1 is the face of P with $1, 2, \ldots l$ as the indices of its corners. To find the rate of exponential decay of P_f, we calculate

$$\begin{aligned} \psi_{tot} &= \frac{1}{n} \log(P_f) \\ &\leq \frac{1}{n} \log(\binom{n-k}{l-k}) + (\gamma - \delta)\log(2) + \psi_{int}(\delta, \gamma) + \psi_{ext}(\gamma) + o(1), \end{aligned}$$

where ψ_{int} and ψ_{ext} are defined in equations 3.6 and 3.8 respectively. We call ψ_{tot} the total exponent and it serves as the exponent of the probability of failure P_f. Whenever $\delta = \frac{k}{n}$ is such that $\psi_{tot} < 0$, the probability of failure of weighted ℓ_1-minimization to recover $x \in F_0$ decays exponentially with respect to the size of the signal n.

Using Stirling approximation for factorials, the exponent of the combinatorial term can be easily found.

$$\frac{1}{n}\log(\binom{n-k}{l-k}) \to \delta H\left(\frac{\gamma-\delta}{1-\delta}\right),$$

where $H(x)$ is the standard entropy function with base e. This gives us a bound on the total exponent

$$\frac{1}{n}\log(P_f) \leq (1-\delta)H\left(\frac{\gamma-\delta}{1-\delta}\right) + \psi_{int} + \psi_{ext} + o(1).$$

However this bound is a strict upper bound on the decay exponent, and can often be loose as for example in the case of linearly varying weights. To improve on the tightness of the bound, we can use a simple technique. Divide the set of indices $k+1, \ldots n$ into 2 parts with $T_1 = \{k+1, \ldots, \frac{n+k}{2}\}$ and $T_2 = \{\frac{n+k}{2}+1, \ldots, n\}$ For a particular l, let G have l_1 vertices in T_1 and l_2 vertices in T_2. Using the same arguement as before, among all faces G with the values of l_1 and l_2 specified as above, the choice that maximizes $\beta(F,G)$ and $\gamma(G,P)$ is the face G with vertices given by the indices $1, \ldots, l_1, \frac{n+k}{2}+1, \ldots, \frac{n+k}{2}+l_2$. Using this we get a revised upper

bound on P_f as

$$P_f \leq \sum_{l=m+1}^{n} \sum_{l_1+l_2=l} \binom{\frac{n-k}{2}}{l_1} \binom{\frac{n-k}{2}}{l_2} \beta(F,G)\gamma(G,P)$$
$$\leq (n-m)(l+1)\binom{\frac{n-k}{2}}{l_1} \binom{\frac{n-k}{2}}{l_2} \beta(F,G_2)\gamma(G_2,P),$$

where the face G_2 is the one obtained by maximizing the expression over $l_1 + l_2 = l$. Define $\gamma_1 = \frac{l_1}{n}$ and $\gamma_2 = \frac{l_2}{n}$. Then the revised bound on the exponent of P_f can be obtained as

$$\frac{1}{n}\log(P_f) \leq \frac{1-\delta}{2} H\left(\frac{2\gamma_1}{1-\delta}\right) + \frac{1-\delta}{2} H\left(\frac{2\gamma_2}{1-\delta}\right) + \psi_{int}(\delta,\gamma_1,\gamma_2) + \psi_{ext}(\gamma_1,\gamma_2) + o(1).$$

We call the term $\frac{1-\delta}{2} H\left(\frac{2\gamma_1}{1-\delta}\right) + \frac{1-\delta}{2} H\left(\frac{2\gamma_2}{1-\delta}\right)$ the *combinatorial exponent* and denote it by $\psi_{com}(\delta,\gamma_1,\gamma_2)$. We can similarly define the face G_i corresponding to dividing the indices denoted by $k+1,\ldots,n$ into p parts and compute the corresponding bound. This gives us method to control the trade-off between the tightness of the bound and the amount of computation it needs. This is described in detail in the next section.

3.4 Improving the Bound on the Exponents

We seek to generalize the method described in the previous section to improve the upper bound on the probability of error. Divide the interval $[\delta, 1]$ into r equal parts. Assume that the face G has l_i indices in the i^{th} interval created by this division. Define $\gamma_i = \frac{l_i}{n}$. Also let $\alpha_i = r\gamma_i$. Following the same procedure as in the previous

section, the upper bound on the exponent of P_f is given by

$$\frac{1}{n}\log(P_f) \leq \max_{\alpha} \psi_{com}(\alpha) + \psi_{int}(\alpha) + \psi_{ext}(\alpha) + o(1),$$

where $\alpha = (\alpha_1, \ldots, \alpha_r)^t$ and α_i is as defined above with $0 \leq \alpha_i \leq \frac{1-\delta}{r}$.

Using the way the exponents were expressed, the problem of finding the total exponent can be posed as

$$\bar{\psi}_{tot} = \max_{\alpha} \ \psi_{com}(\alpha) + \psi_{int}(\alpha) + \psi_{ext}(\alpha),$$

where

$$\psi_{int}(\alpha) = \max_{y} \ \psi_{int}(\alpha, y),$$

and

$$\psi_{ext}(\alpha) = \max_{x} \ \psi_{ext}(\alpha, x).$$

So, the total exponent, which is the exponent of the upper bound on the probability of failure P_f of the weighted ℓ_1-minimization, is obtained by performing the following maximization:

$$\bar{\psi}_{tot} = \max_{\alpha,x,y} \psi_{tot}(\alpha, x, y), \tag{3.9}$$

where $\psi_{tot}(\alpha, x, y) = \psi_{com}(\alpha) + \psi_{int}(\alpha, y) + \psi_{ext}(\alpha, x)$. Whenever $\delta = \frac{k}{n}$ is such that $\bar{\psi}_{tot} < 0$, the probability of failure of weighted ℓ_1-minimization to recover $x \in F_0$ decays exponentially with respect to the size of the signal n.

We now compute the expressions for each of the functions appearing in the above optimization problem. For the subsequent derivation, we define $f_i = f\left(\delta + \frac{(i-1)(1-\delta)}{r}\right)$.

3.4.1 Combinatorial Exponent

From a direct generalization of the expression at the end of section 6, we get

$$\begin{aligned}\psi_{com} &= \frac{1}{r}\sum_{i=1}^{r}(1-\delta)H\left(\frac{r\gamma_i}{1-\delta}\right) \\ &= \frac{1-\delta}{r}\sum_{i=1}^{r}H\left(\frac{\alpha_i}{1-\delta}\right).\end{aligned}$$

For the internal and external angle exponents, in addition to obtaining their expressions, we will also bound them suitably by analytically simpler expressions so that the optimization problem described in 3.9 becomes more tractable.

3.4.2 External Angle Exponent

The external angle exponent is given by

$$-\psi_{ext}(x) = \zeta(x) = c_2x^2 - \log\left(G_0(x)\right).$$

$$c_2 = \int_0^{\delta} f^2(u)du + \sum_{i=1}^{r}\int_{\delta+\frac{(i-1)(1-\delta)}{r}}^{\delta+\frac{(i-1)(1-\delta)}{r}+\frac{\alpha_i}{r}} f^2(u)du.$$

As $f(.)$ is an increasing function, the integral appearing above in the expression of c_2 can be bound by its left Riemann sum.

$$c_2 \geq \int_0^{\delta} f^2(u)du + \frac{1}{r}\sum_{i=1}^{r} f_i^2\alpha_i \triangleq \bar{c_2}.$$

Similary,

$$\begin{aligned}\log(G_0(x)) &= \int_{\delta}^{1} \log(\text{erf}(xf(u)))du - \sum_{i=1}^{r}\int_{\delta+\frac{(i-1)(1-\delta)}{r}}^{\delta+\frac{(i-1)(1-\delta)}{r}+\frac{\alpha_i}{r}} \log(\text{erf}(xf(u)))du \\ &\leq \int_{\delta}^{1} \log(\text{erf}(xf(u)))du - \frac{1}{r}\sum_{i=1}^{r}\log(\text{erf}(xf_i)) \triangleq \log(\bar{G_0}(x)).\end{aligned}$$

So,

$$\zeta(x) \geq \bar{c_2}x^2 - \log(\bar{G_0}(x)) \triangleq \bar{\zeta(x)}.$$

3.4.3 Internal Angle Exponent

The internal angle exponent is given by

$$-\psi_{int}(y) = \eta(y) = \frac{c_0^2}{2c_1}y^2 + c_0\lambda_0^*(y),$$

where,

$$\begin{aligned}c_0 &= \sum_{i=1}^{r}\int_{\delta+\frac{(i-1)(1-\delta)}{r}}^{\delta+\frac{(i-1)(1-\delta)}{r}+\frac{\alpha_i}{r}} f(u)du \\ &\geq \frac{1}{r}\sum_{i=1}^{r} f_i\alpha_i \triangleq \bar{c_0}.\end{aligned}$$

$\lambda_0^*(y)$ is the convex conjugate of $\lambda_0(.)$ and is given by,

$$\lambda_0^*(y) = \max_s \ sy - \lambda_0(s).$$

We are interested in only in the region $s \leq 0$. In this region we have,

$$\begin{aligned}\lambda_0(s) &= \sum_{i=1}^{r} \int_{\delta+\frac{(i-1)(1-\delta)}{r}}^{\delta+\frac{(i-1)(1-\delta)}{r}+\frac{\alpha_i}{r}} \lambda(sf(u))du \\ &\leq \sum_{i=1}^{r} \lambda(sf_i) \triangleq \bar{\lambda}_0(s),\end{aligned}$$

which follows from the fact that $s \leq 0$ and $\lambda(u)$ is an increasing function of u. This gives

$$\max_s \ sy - \lambda_0(s) \geq \max_s \ sy - \bar{\lambda}_0(s),$$

and hence

$$\lambda_0^*(y) \geq \bar{\lambda}_0^*(y) = \max_s \ sy - \bar{\lambda}_0(s).$$

So, we conclude

$$\eta(y) \geq \frac{\bar{c}_0^2}{2c_1} y^2 + \bar{c}_0 \bar{\lambda}_0^*(y) \triangleq \bar{\eta}(y).$$

As we seek to maximize the sum of the exponents with respect to α, it would be of interest to study the curvature properties of the functions. This is the topic of the next section. However, we present in advance the variation of the value of the maximum recoverable δ as computed by the methods of this section with respect

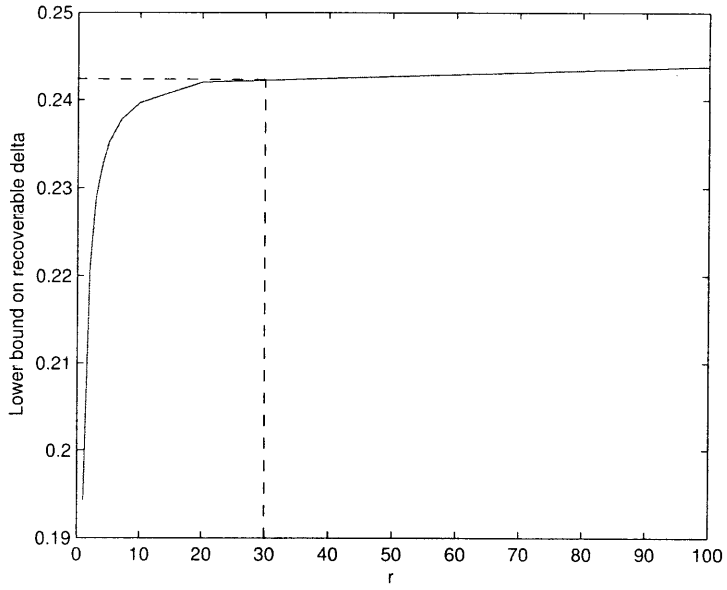

Figure 3-1: Maximum recoverable δ vs r computed using the methods of this section.

to the parameter r which controls the accuracy of the method. For this, we fix a compression ratio $\frac{m}{n} = 0.5$. The weights w_i are chosen as $w_i = 1 + \frac{i}{n}$. Figure 3-1 demonstrates this dependence. Note how the bound improves with increasing value of r.

3.5 Concavity of the Exponent Functions

In this section, we will show that the function $\psi_{tot}(\alpha, x, y)$ to be maximized that appears in the definition of the total exponent in equation (3.9) is concave in α for fixed x and y. This indicates that the maximization with respect to α can be carried

out efficiently. The combinatorial exponent function is given by

$$\psi_{com} = \frac{1-\delta}{r} \sum_{i=1}^{r} H\left(\frac{\alpha_i}{1-\delta}\right)$$

and is clearly a concave function of α. The external angle exponent is given by

$$-\psi_{ext}(x,\alpha) = \zeta(x) = c_2 x^2 - \log(G_0(x)).$$

As c_2 and $\log(G_0(x)$ are both linear functions of α, the external angle exponent is a linear function of α for a fixed value of x.

The internal angle exponent needs a bit more work to prove its concavity. We analyze the curvature of the Internal angle exponent with respect to α for a fixed value of y.

$$-\psi_{int}(y,\alpha) = \eta(y,\alpha) = \frac{c_0^2}{2c_1} y^2 + c_0 \lambda_0^*(y).$$

$c_0 = \frac{1}{r}\sum_{i=1}^{r} f_i\alpha_i$ is a linear function of α and hence $\frac{c_0^2}{2c_1}y^2$ is a convex quadratic function of α.

$$\lambda_0^*(y) = \max_s \; sy - \lambda_0(s) = s^* y - \lambda_0(s^*).$$

where s^* is the maximizing s and is characterized by

$$\lambda_0^{'}(s^*) = y \tag{3.10}$$

$$\Longrightarrow \sum_{i=1}^{r} f_i\alpha_i\lambda^{'}(sf_i) = c_0 y. \tag{3.11}$$

Differentiating the above equation with respect to α_i gives

$$\left(\sum_{j=1}^{r} f_j^2 \alpha_j \lambda^{''}(sf_j)\right) \frac{\partial s^*}{\partial \alpha_i} + f_i \lambda^{'}(sf_i) = f_i y, \quad 1 \leq i \leq r. \tag{3.12}$$

Now we consider the second term which is given by

$$F(\alpha) = c_0 \lambda_0^*(y) = c_0 s^* y - \sum_{i=1}^{r} \alpha_i \lambda(s^* f_i).$$

Differentiating,

$$\begin{aligned} \frac{\partial F}{\partial \alpha_i} &= \frac{\partial c_0}{\partial \alpha_i} s^* y + \frac{\partial s^*}{\partial \alpha_i} c_0 y \\ &\quad - \left(\sum_{j=1}^{r} f_j \lambda^{'}(s^* f_j)\right) \frac{\partial s^*}{\partial \alpha_i} - \lambda(s^* f_i). \end{aligned}$$

By using 3.11,

$$\frac{\partial F}{\partial \alpha_i} = f_i s^* y - \lambda(s^* f_i)$$

Differentiating with respect to α_j,

$$\begin{aligned} \frac{\partial^2 F}{\partial \alpha_i \alpha_j} &= \left(f_i y - f_i \lambda^{'}(s^* f_i)\right) \frac{\partial s^*}{\partial \alpha_j} \\ &= \left(\sum_{j=1}^{r} f_j^2 \alpha_j \lambda^{''}(sf_j)\right) \frac{\partial s^*}{\partial \alpha_i} \frac{\partial s^*}{\partial \alpha_j}. \end{aligned}$$

where the last line follows from 3.12. As $\lambda(.)$ is a convex function, the quantity $\sum_{j=1}^{r} f_j^2 \alpha_j \lambda^{''}(sf_j)$ is positive, which we can represent by $\sum_{j=1}^{r} f_j^2 \alpha_j \lambda^{''}(sf_j) = c^2$ for

some $c > 0$. So the Hessian matrix of F with respect to α is given by

$$\frac{\partial^2 F}{\partial \alpha^2} = (cDs^*)(cDs^*)' \succeq 0,$$

where Ds^* denotes the gradient vector of s^* with respect to α. This proves that the function $\eta(y, \alpha)$ is a convex function of α for a fixed y. So, we conclude that

$$\psi_{tot}(x, y, \alpha) = \psi_{com}(\alpha) + \psi_{int}(\alpha, y) + \psi_{ext}(\alpha, x)$$

is a concave function of α for given x, y.

3.6 Incorporating the probabilities in the derivation.

Until now, we focused on studying the properties of the face F_0 defined by the corners $\frac{1}{w_1}e_1, \ldots, \frac{1}{w_k}e_k$ under the random projection A. We showed that whenever $\delta = \frac{k}{n}$ is such that $\bar{\psi}_{tot} < 0$, the probability of failure of weighted ℓ_1-minimization to recover $x \in F_0$ decays exponentially with respect to the size of the signal n.

We now return to the problem of recovering sparse signals sampled from a given probabilistic model using weighted ℓ_1-minimization. Straight-forward generalizations of the analysis and expressions derived in the previous sections will be extremely useful for us to study this problem. We begin by trying to bound the probability of error by exponential functions. We subsequently define a certain notion of epsilon typicality, which will allow us to consider the performance of weighted ℓ_1-minimization only for "typical" vectors x.

3.6.1 Bounding the probability of error and ϵ-typicality

Let $p : [0,1] \to \mathbb{R}^+$ be a continuous and monotonically decreasing function. Let the probability of the i^{th} component of x being non-zero be given by, $p_i = p\left(\frac{i}{n}\right)$. We can also always normalize the vector x so that it lies on one of the faces of the weighted ℓ_1 ball. The probabilities p_i then directly allow us to associate with each face, the probability of x being on that face. Specifically, if the indices of the corner of the face F are $r_1, r_2, \ldots, r_k$, then the probability associated with it is given by, $Pr(F) = \prod_{i=1}^{k} p_{r_i}$. We divide the set of indices from $1, 2, \ldots, n$ into r equal parts as before creating p different intervals of indices which we denote by $I_1, I_2, \ldots, I_p$. We denote by $J(k_1, k_2, \ldots, k_p)$ the set of all faces of the polytope with k_i indices in the i^{th} interval of indices.

Let E denote the event that the weighted ℓ_1-minimization does not produce the correct solution. Then we have

$$\mathbf{P}(E) = \sum_{k_1,k_2,\ldots,k_r} \sum_{F \in J(k_1,k_2,\ldots,k_r)} \mathbf{P}(F)\mathbf{P}(E|F). \tag{3.13}$$

We can just consider one representative among the $2^{\sum_i k_i}$ faces created by the different sign patterns. This is because, by the symmetry of the problem, all the faces in a particular class of faces defined by $k_1, k_2, \ldots, k_r$ have the same probabilities $\mathbf{P}(F)$ and $\mathbf{P}(E|F)$. Let the set of indices representing the face F be denoted by $I(F)$. For a given value of $k_1, k_2, \ldots, k_r$, $|I(F) \cap I_i| = k_i$. Also let $k_i = \frac{g_i}{r} n$. Then

$$\mathbf{P}(F) = \left(\prod_{i=1}^{r} \prod_{j \in I(F) \cap I_i} \frac{p(j/n)}{1 - p(j/n)} \right) \prod_{i=1}^{n} (1 - p(j/n)).$$

The function $\frac{x}{1-x}$ is an increasing function of x for $x \in (0,1)$. So,

$$\mathbf{P}(F) \leq \left(\prod_{i=1}^{r} \left(\frac{p\left(\frac{i-1}{r}\right)}{1-p\left(\frac{i-1}{r}\right)} \right)^{k_i} \right) \prod_{i=1}^{n} (1-p(j/n)).$$

Denote the right hand side of the above inequality be $P(k_1, k_2, \ldots, k_r)$. Among all faces $F \in J(k_1, k_2, \ldots, k_r)$, the one which maximizes $\mathbf{P}(E|F)$ is the one obtained by stacking all the indices to the right of each interval. We denote this maximum probability by $P(E|(k_1, k_2, \ldots, k_r))$. Combining the above two we get

$$\begin{aligned} \mathbf{P}(E) &\leq \sum_{k_1,k_2,\ldots,k_r} \sum_{F \in J(k_1,k_2,\ldots,k_r)} P(k_1, k_2, \ldots, k_r) P(E|(k_1, k_2, \ldots, k_r)) \\ &= \sum_{k_1,k_2,\ldots,k_r} \left(\prod_{i=1}^{r} \binom{\frac{n}{r}}{\frac{g_i}{r}n} \right) P(k_1, k_2, \ldots, k_r) P(E|(k_1, k_2, \ldots, k_r)). \end{aligned} \tag{3.14}$$

Define the quantity $SP(k_1, k_2, \ldots, k_r)$ as

$$SP(k_1, k_2, \ldots, k_r) \triangleq \left(\prod_{i=1}^{r} \binom{\frac{n}{r}}{\frac{g_i}{r}n} \right) P(k_1, k_2, \ldots, k_r).$$

The above quantity serves as an upper bound on the probability of the event that the signal x has k_i non-zero elements in the i^{th} interval. Using this we rewrite the inequality (3.14) as

$$\mathbf{P}(E) \leq \sum_{k_1,k_2,\ldots,k_r} SP(k_1, k_2, \ldots, k_r) P(E|(k_1, k_2, \ldots, k_r)). \tag{3.15}$$

As the function $p(u)$, which defines the probability of each entry of x being non-zero ($\mathbf{P}(x \neq 0) = r\left(\frac{i}{n}\right)$), is monotonically decreasing in u, one might expect that all

the terms, for different values of $k_1, k_2, \ldots, k_r$ do not contribute equally to the sum in the right hand side of (3.13). In what follows, we will show that we need to focus our attention only to a certain "typical" set of values of $k_1, k_2, \ldots, k_r$ to compute the exponent of the probability of error $\mathbf{P}(E)$. The following definition helps us define precisely what this "typical" set of $k_1, k_2, \ldots, k_r$ is.

Definition 3.6.1. For a fixed value of r, let $\Delta(r) = \int_0^1 \log(1-p(u))du - \frac{1}{r}\sum_{i=1}^r \log(1-p\left(\frac{i-1}{r}\right))$. Define $q = (q_1, \ldots, q_r)^T$ to be $\epsilon - typical$ if the following conditions are satisfied.

1. $\frac{1}{r}\sum_{i=1}^r D(q_i||p_i) \leq \epsilon + \Delta(r)$.
2. $|\frac{1}{r}\sum_{i=1}^r q_i - \int_0^1 p(x)dx| \leq \epsilon$.

We state and prove certain lemmas that will justify the above definition for ϵ-*typicality*.

Lemma 3.6.1. *Let $D(q||p)$ denotes the Kullback-Leibler distance between two Bernoulli random variables with probability of success given by q and p respectively. If we have $\frac{1}{r}\sum_{i=1}^r D(q_i||p_i) > \epsilon + \Delta(m)$, then there exists n_0, such that for all $n > n_0$,*

$$SP(k_1, \ldots, k_r) < e^{-b(\epsilon)n},$$

where $b(\epsilon)$ is a positive constant.

Proof. We have

$$SP(k_1, k_2, \ldots, k_r) = \left(\prod_{i=1}^r \binom{\frac{n}{r}}{\frac{q_i}{r}n}\right) P(k_1, k_2, \ldots, k_r).$$

Then,

$$\frac{1}{n}\log(SP(k_1,k_2,\ldots,k_r)) = \frac{1}{n}\sum_{i=1}^{r}\binom{\frac{n}{r}}{\frac{g_i n}{r}} + \frac{1}{n}\log(P(k_1,k_2,\ldots,k_r))$$
$$= \frac{1}{n}\sum_{i=1}^{r}\binom{\frac{n}{r}}{\frac{g_i n}{r}} + \frac{1}{n}\sum_{i=1}^{r}\frac{g_i n}{r}\log\left(\frac{p_i}{1-p_i}\right) + \frac{1}{n}\sum_{j=1}^{n}\log\left(1-p\left(\frac{j}{n}\right)\right).$$

Letting $n \to \infty$,

$$\lim_{n\to\infty}\frac{1}{n}\log(SP(k_1,k_2,\ldots,k_r))$$
$$=\frac{1}{r}\sum_{i=1}^{r}H(g_i) + \frac{1}{r}\sum_{i=1}^{r}g_i\log\left(\frac{p_i}{1-p_i}\right)$$
$$+\int_0^1\log(1-p(u))du$$
$$=\frac{1}{r}\sum_{i=1}^{r}H(g_i) + (g_i\log(p_i) + (1-g_i)\log(1-p_i)) - \log(1-p\left(\frac{i-1}{r}\right))$$
$$+\int_0^1\log(1-p(u))du$$
$$=\frac{1}{r}\sum_{i=1}^{r}-D(q_i||p_i) + \left[\int_0^1\log(1-p(u))du - \frac{1}{r}\sum_{i=1}^{r}\log(1-p\left(\frac{i-1}{r}\right))\right].$$

If the condition given in the lemma is satisfied, then

$$\lim_{n\to\infty}\frac{1}{n}\log(SP(k_1,k_2,\ldots,k_r)) < -\epsilon.$$

The claim in the lemma then follows. □

Lemma 3.6.2. *Let Q_β denote the event that the average number of non-zero elements*

of x is β, i.e. $\frac{1}{n}|supp(x)| = \beta$. Let $\delta = \int_0^1 p(x)dx$. Then,

$$\lim_{n\to\infty} \frac{1}{n} \log(\mathbf{P}(Q_\beta)) \leq -D(\beta||\delta).$$

In particular if $|\beta - \delta| > \epsilon$ for some $\epsilon > 0$, then there exists n_0 such that for all $n > n_0$,

$$\mathbf{P}(|\frac{1}{n}|supp(x)| - \int_0^1 p(x)dx\,| > \epsilon) < e^{-a(\epsilon)n},$$

where $a(\epsilon)$ is a positive constant.

Proof. Divide the indices $1, \ldots, n$ into m parts and define I_i as in section 3.6.1. Let $\beta_i = \frac{r}{n}|supp(x) \cap I_i|$. Following the derivation as in the proof of lemma 3.6.1 we get,

$$\mathbf{P}(Q_\beta) \leq (n + r - 1)^{r-1} \left(\prod_{i=1}^{r} \binom{\frac{n}{r}}{\frac{\beta_i}{r}n} \right) P\left(\frac{n}{r}\beta_1, \frac{n}{r}\beta_2, \ldots, \frac{n}{r}\beta_r\right).$$

where $\frac{1}{r}\sum_{i=1}^{r} \beta_i = \beta$. This gives us,

$$\lim_{n\to\infty} \frac{1}{n} \log(\mathbf{P}(Q_\beta)) \leq \frac{1}{r} \sum_{i=1}^{r} -D(\beta_i||p\left(\frac{i-1}{r}\right))+$$
$$\left[\int_0^1 \log(1 - p(u))du - \frac{1}{r}\sum_{i=1}^{r} \log(1 - p\left(\frac{i-1}{r}\right))\right].$$

Let $p_{i,r} = p\left(\frac{i-1}{r}\right))$. We consider the term

$$\sum_{i=1}^{r} D(\beta_i||p\left(\frac{i-1}{r}\right)) = \left(\sum_{i=1}^{r} \beta_i \log(\beta_i/p_i)\right) + \left(\sum_{i=1}^{r} (1 - \beta_i) \log((1 - \beta_i)/(1 - p_i))\right).$$

Using the log-sum inequality, we obtain,

$$\frac{1}{r}\sum_{i=1}^{r} D(\beta_i||p\left(\frac{i-1}{r}\right)) \geq \left(\frac{\sum_{i=1}^{r}\beta_i}{r}\right)\log\left(\frac{\sum_{i=1}^{r}\beta_i}{\sum_{i=1}^{r}p_i}\right) + \left(\frac{\sum_{i=1}^{r}1-\beta_i}{r}\right)\log\left(\frac{\sum_{i=1}^{r}1-\beta_i}{\sum_{i=1}^{r}1-p_i}\right).$$

Define $p_{s,r} = \frac{1}{r}\sum_{i=1}^{r} p\left(\frac{i-1}{r}\right)$. So,

$$\frac{1}{r}\sum_{i=1}^{r} D(\beta_i||p\left(\frac{i-1}{r}\right)) \geq D(\beta||p_{s,r}).$$

Using the above,

$$\lim_{n\to\infty}\frac{1}{n}\log(\mathbf{P}(Q_\beta)) \leq -D(\beta||p_{s,r}) + \left[\int_0^1 \log(1-p(u))du - \frac{1}{r}\sum_{i=1}^{r}\log(1-p\left(\frac{i-1}{r}\right))\right].$$

As the above is true for every r, we let $r \to \infty$ to get

$$\lim_{n\to\infty}\frac{1}{n}\log(Pr\{Q_\beta\}) \leq -D(\beta||\delta),$$

which follows from

$$\lim_{r\to\infty}\int_0^1 \log(1-p(u))du - \frac{1}{r}\sum_{i=1}^{r}\log(1-p\left(\frac{i-1}{r}\right)) = 0, \text{ and}$$

$$\lim_{r\to\infty} p_{s,r} = \lim_{r\to\infty}\frac{1}{r}\sum_{i=1}^{r} p\left(\frac{i-1}{r}\right) = \int_0^1 p(u)du = \delta.$$

If the premise of the lemma is satisfied, then we have $D(\beta||\delta) > \bar{b}(\epsilon)$. The claim in the lemma then follows. □

We now retrace our derivation from equation (3.13). Using the definition of

ϵ-typicality, we can write

$$\mathbf{P}(E) = \underbrace{\sum_{(k_1,k_2,\ldots,k_r \text{ is } \epsilon \text{ typical})} \sum_{(F \in J(k_1,k_2,\ldots,k_r))} \mathbf{P}(F)\mathbf{P}(E|F).}_{I} +$$
$$\underbrace{\sum_{(k_1,k_2,\ldots,k_r \text{ not } \epsilon \text{ typical})} \sum_{(F \in J(k_1,k_2,\ldots,k_r))} \mathbf{P}(F)\mathbf{P}(E|F)}_{II}.$$

For a fixed value of m, the number of possible values of $k_1, k_2, \ldots, k_r$ is bounded by $n(n+r-1)^{r-1}$. Also,

$$\sum_{(F \in J(k_1,k_2,\ldots,k_r))} \mathbf{P}(F)\mathbf{P}(E|F) \leq SP(k_1,\ldots,k_r).$$

So, the second term II, can be bounded as

$$II \leq n(n+r-1)^{r-1} e^{-c(\epsilon)n},$$

for some positive constant $c(\epsilon)$. As $\lim_{n\to\infty} \frac{1}{n} \log\left(n(n+r-1)^{r-1}\right) = 0$, there exists n_0, such that for all $n > n_0$,

$$II \leq e^{-c_0(\epsilon)n},$$

for some positive constant $c_0(\epsilon)$. This allows us to only consider the first term I. Among all $k_1, \ldots, k_m$ *ϵ-typical*, let $F^* \in J(k_1^*, \ldots, k_r^*)$ be the face which maximizes the probability $\mathbf{P}(E|F)$. Then

$$I \leq n(n+r-1)^{r-1} \mathbf{P}(E|F^*).$$

This gives

$$\lim_{n\to\infty} \frac{1}{n} \log(I) \leq \lim_{n\to\infty} \frac{1}{n} \log(\mathbf{P}(E|F^*)).$$

In the next subsection we use the techniques developed earlier to compute the angle exponents and thus providing sufficient conditions under which weighted ℓ_1-minimization yields the correct solution with overwhelming probability.

3.6.2 Exponents

To bound $\mathbf{P}(E|F)$, we use the same procedure as was used in section 4. For a face F described by $k_1, \ldots, k_m$ as in the previous section, we define $g = (g_1, \ldots, g_r)^T$, where $g_i = k_i \frac{r}{n}$. As the method is identical to before, we just give the final expressions for the combinatorial, internal and external angle exponents for a given value of $g = (g_1, g_2, \ldots, g_r)^T$.

Combinatorial Exponent

$$\psi_{com} = \frac{1}{r} \sum_{i=1}^{r} (1 - g_i) \log \left(\frac{h_i}{1 - g_i} \right).$$

Internal Angle Exponent

$$-\psi_{int}(y) = \eta(y) = \frac{c_0^2}{2c_1} y^2 + c_0 \lambda_0^*(y),$$

where

$$c_0 = \frac{1}{r}\sum_{i=1}^{r} f_i h_i,$$

$$c_1 = \frac{1}{r}\sum_{i=1}^{r} f_i^2 g_i,$$

$$\lambda_0^*(y) = \max_s sy - \lambda_0(s),$$

$$\lambda_0(s) = \frac{1}{r}\sum_{i=1}^{r} \frac{1}{c_0}\lambda(sf_i)(h_i).$$

External Angle Exponent

$$-\psi_{ext}(x) = \zeta(x) = c_2 x^2 - \log(G_0(x)),$$

where,

$$c_2 = \frac{1}{r}\sum_{i=1}^{r} f_i^2(g_i + h_i),$$

$$\log(G_0(x)) = \int_0^1 \log(G(xf(u)))du - \frac{1}{r}\sum_{i=1}^{r} \log(G(xf_i))(h_i + g_i).$$

Total Exponent

Combining the exponents and using the results in section 3.6.1

$$\frac{1}{n}\log(\mathbf{P}(E)) \leq \bar{\psi}_{tot} + o(1).$$

where $\bar{\psi}_{tot}$ is obtained by solving the following optimization problem.

$$\begin{aligned} \max_{g,h,x,y} \quad & \psi_{com} + \psi_{int}(y) + \psi_{ext}(x) \\ \text{subject to} \quad & \frac{1}{r}\sum_{i=1}^{r} D(q_i||p_i) < \Delta(r), \\ & \frac{1}{r}\sum_{i=1}^{r} q_i = \delta. \end{aligned}$$

Chapter 4

Numerical Computations and Simulations

In this chapter, we compute the bounds using the techniques developed in Chapter 3 for certain specific probability function $p(.)$ and weight function $f(.)$. In particular we consider

$$p(u) = \delta - c(u - 0.5), \quad u \in [0, 1],$$
$$f(u) = 1 + \rho u, \quad u \in [0, 1].$$

Before proceeding to evaluation of the performance of weighted ℓ_1-minimization in the problem specified by the above choice of functions, we will first present theoretical bounds and simulations related to the behavior of the so-called *first face* F_0, as described in section 3.1 when the corresponding cross-polytope is described by the function $f(.)$. This is contained in section 4.1. The overall performance evaluation is delayed till section 4.2.

4.1 Behavior of F_0 under random projection.

Recall that, for a given set of weights, the weighted ℓ_1-ball is the cross polytope in n dimensions whose corners in the first quadrant are given by $\frac{e_1}{w_1}, \ldots, \frac{e_k}{w_n}$. The face F_0 of the weighted ℓ_1-ball is defined by the vertices $\frac{e_1}{w_1}, \ldots, \frac{e_k}{w_k}$. In Chapter 3, we developed methods to compute a lower bound on the threshold $\bar{\delta} = \frac{k}{n}$ below which the face F_0 survives a random projection defined by a matrix $A \in \mathbb{R}^{m \times n}$ with overwhelming probability. This also corresponds to the event when weighted ℓ_1-minimization recovers a signal x whose support is the first k indices. In view of our choice of weights, which is described by the function $f(u) = 1 + \rho u$ with $\rho \geq 0$, higher values of ρ correspond to more steeply varying weights. Intuitively, one may expect that higher values of ρ, will make the weighted ℓ_1 norm cost function favor non-zero entries in the first few indices. This may allow the threshold $\bar{\delta}$ to be larger.

We will show, the lower bound on $\bar{\delta}$ we suggested follows an increasing trend as described above. To demonstrate this for a certain choice of the parameters, we fix the compression ratio $\frac{m}{n} = 0.5$ and compute the lower bound using the methods developed in Chapter 3. Based on figure 3-1 we choose $r = 30$ as a reasonable value in our computations. Figure 4-1, shows the dependence of this threshold on the value of ρ which determines the weight function $f(.)$. The value of the bound at $\rho = 0$ corresponds to the case when F_0 is a face of the regular ℓ_1 ball. Not surprisingly this matches the value reported earlier in [7].

To evaluate the accuracy of the bound, we then compare the values of the threshold predicted by the lower bound to that obtained empirically through simulations for two different values of the parameter ρ. For this, we set $m = 200, n = 400$, and obtain the fraction of times the face F_0 failed to survive a random projection from a total of 100 iterations. This is done by randomly generating a vector x for each

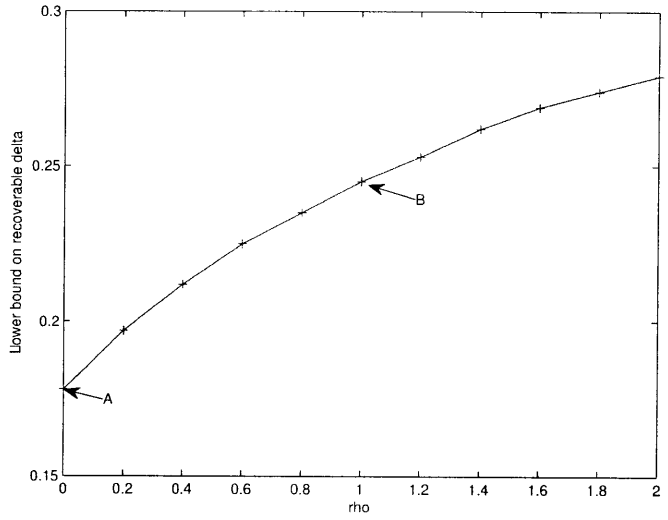

Figure 4-1: Lower bound on maximum recoverable δ vs ρ for the "first face" F_0, computed using the methods developed in Chapter 3 for $r = 30$

iteration with support $1, \ldots, k$ and using weighted ℓ_1-minimization to recover that x from its measurements given by $y = Ax$. Figure 4-2 and Figure 4-3 show this plot for $\rho = 0$ and $\rho = 1$ respectively. The vertical lines in the plots (marked A and B respectively) denote the lower bounds corresponding to the value of ρ in figure 4-1. The simulations show a rapid fall in P_f around the theoretical lower bound as we decrease the value of δ. This indicates that the lower bounds developed are fairly tight.

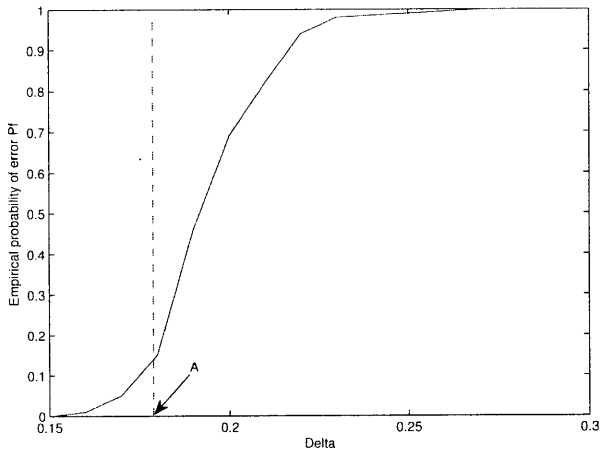

Figure 4-2: Empirical probability of error P_f vs δ with $\rho = 0$ for F_0 obtained through simulations using m = 200, n = 400 and 100 iterations. The vertical line refers to the lower bound computed using methods of Chapter 3.

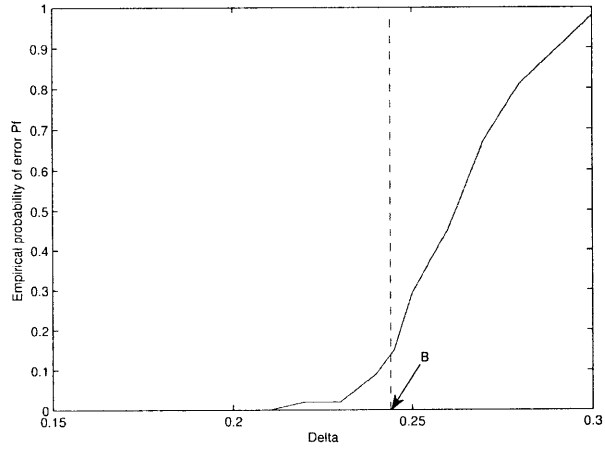

Figure 4-3: Empirical probability of error P_f vs δ with $\rho = 1$ for F_0 obtained through simulations using m = 200, n = 400 and 100 iterations. The vertical line refers to the lower bound computed using methods of Chapter 3.

4.2 Performance of weighted ℓ_1-minimization.

We consider that the function $p(.)$ defining the probabilities is given by

$$p(u) = \delta - c(u - 0.5), \quad u \in [0, 1], c \geq 0.$$

The expected level of sparsity is then given by δ. To recover the sparse signal, we use weighted ℓ_1-minimization with weights defined by the weight function $f(x) = 1 + \rho x$. Of course, the choice of ρ plays an important role in the success of weighted ℓ_1-minimization and it would be of interest to be able to obtain the value of ρ corresponding to the value of c for which one gets best performance. One way to estimate the effect of ρ is to compute the lower bound on the threshold δ as suggested in Chapter 3 and observe the trend. The value of the lower bound however also depends on the parameter m, which controls the tightness of the bound. While higher values of m allows us to get a tighter bound, it also increases the computational power requirement for obtaining the bound. So, it is of interest to know how the value of the bound changes with the parameter m.

We fix the ratio $\frac{m}{n} = 0.5$ and compute the lower bound on recoverable δ (which denotes the expected fraction of non-zero components of the signal) using the methods developed in Chapter 3. The accuracy parameter r is fixed at 30. Figure 4-4, shows the dependence of this threshold on the values of ρ for two different values of c. The curves suggest that for larger values of c, which correspond to more rapidly decaying probabilities. the value of $\rho = \rho^*(c)$ which maximizes the lower bound is also higher. At the same time, the value of the lower bound evaluated at $\rho = \rho^*(c)$ also increases with increasing c. This suggests that rapidly decaying probabilities allow us to recover less sparse signals by using an appropriate weighted ℓ_1-minimization.

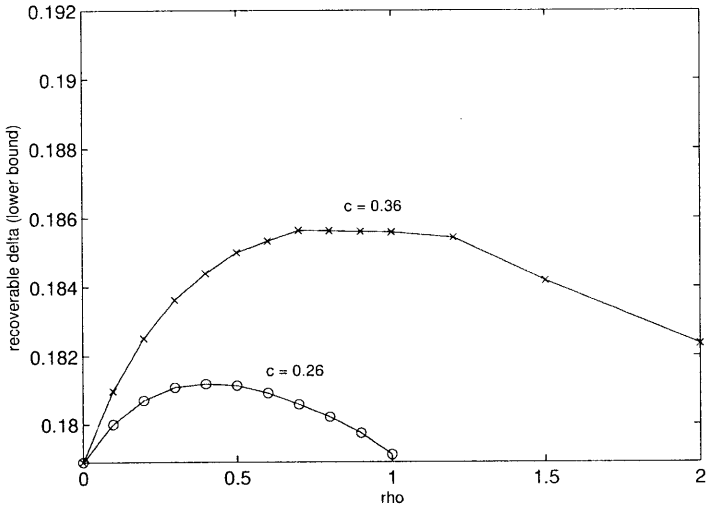

Figure 4-4: Lower bound on recoverable δ vs ρ for $\frac{m}{n} = 0.5$ computed using the methods of Chapter 3, for $c = 0.26$ and $c = 0.36$. The parameter r is fixed at 30.

To observe the effect of m on the value of the lower bound, we plot the same curves as described above for $r = 60$. We remarked earlier that higher values of m allows us to compute tighter bounds. This can be observed from figure 4-5, where we can see that the curves representing the lower bounds show larger values than those in figure 4-4.

Now, we aim at evaluating the performance of weighted ℓ_1-minimization empirically. The value of δ is fixed at 0.185. We then choose a value of c which fixes the probability function $p(.)$. We sample random signals with supports generated by the distribution imposed by $p(.)$. We then make use of the curves for lower bound computed for figure 4-5 to make the best choice of ρ (see table 4.1) and use weighted ℓ_1-minimization corresponding to this ρ to recover the generated signal from its measurements. The failure fraction of this method is computed over 500 iterations. The values of m and n are chosen to be 500 and 1000 respectively. To compare the per-

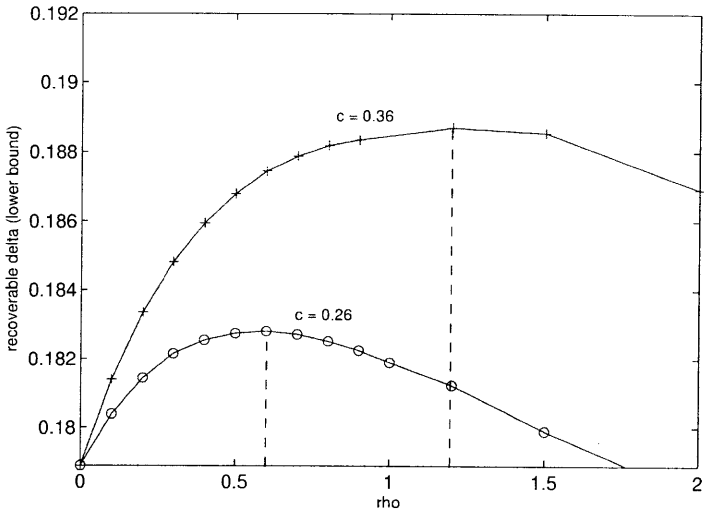

Figure 4-5: Lower bound on recoverable δ vs ρ for $\frac{m}{n} = 0.5$ computed using the methods of Chapter 3, for $c = 0.26$ and $c = 0.36$. The parameter r is fixed at 60.

formance of weighted ℓ_1-minimization to standard ℓ_1-minimization, we repeat the same procedure but use standard ℓ_1-minimization to recover the signal. Figure 4-6 compares the values generated by each method. Notice how the performance of the standard ℓ_1-minimization method remains more or less invariant with increasing c. This shows that it fails to exploit the extra information present in c (i.e. the decaying nature of the probabilities) and its performance depends only on the value of δ, the expected level of sparsity. On the other hand, the performance of weighted ℓ_1-minimization improved with c. This is also in agreement of what is predicted by the lower bounds presented in figure 4-5.

Table 4.1: c vs $\rho^*(c)$ using theoretical lower bounds with $r = 60$ (figure 4-5)

c	0	0.16	0.26	0.36
ρ	0	0.1	0.6	1.2

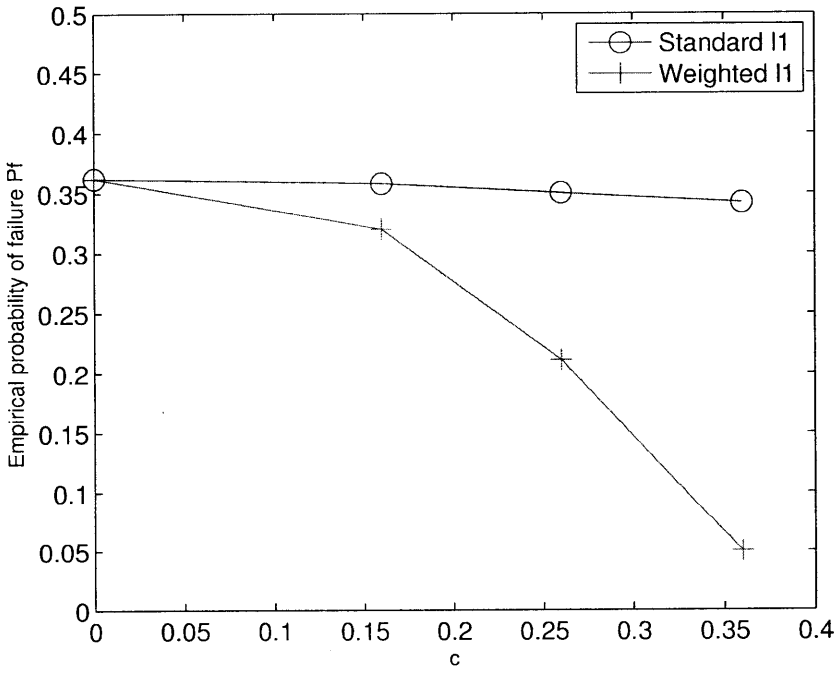

Figure 4-6: Empirical probability of error P_f vs c. Probability function $p(u) = 0.185 - c(u - 0.5)$. Problem size is given by $m = 500$, $n = 1000$. Number of iterations $= 500$.

Chapter 5

Conclusion and Future Work

We gave a brief description of the major results in the Compressed Sensing literature, with special focus on results by Donoho in [7] and Xu in [13]. We outlined the techniques developed to provide sufficient conditions for success of weighted ℓ_1-minimization for model based compressed sensing in a probabilistic setting for the simple class of weights considered in [13]. We posed the problem of providing similar sufficient conditions for a more complex class of weights, namely when the weights are uniform samples of a continuous function. We leveraged the techniques developed in [7] and [13] with our own additions to achieve this. In the process, we also provided conditions under which certain special class of faces of the skewed cross-polytope get "swallowed" under random projections.

There are still certain questions of interest that can be addressed in future work. As we saw, a simple modification to the standard ℓ_1-minimization by incorporating weights is able to accommodate and exploit the additional information provided by the probabilities p_i imposed on the components of the underlying signal x. Can such simple modifications to iterative algorithms like CoSamp and IHT do the same? This

question has been answered in the positive by the authors in [2] for the case of a deterministic model. The question that remains is if this can also be done for a probabilistic model.

Another question we would like to bring up is central to the weighted ℓ_1-minimization based approach. Although it is possible to verify whether for a certain set of probabilities given to us, if a certain choice of weights will guarantee recovery with overwhelming probability, the question of "optimal" weights still remains unanswered. By this we mean, what choice of weights based on the given probabilities, will give us the best performance, or in other words, the least stringent sufficient condition for recovery. In this thesis, the choice of linear family weights for linearly decaying probabilities was based on intuition derived from simulations. However, it would be greatly useful to be able to analytically predict best choice of weights.

Bibliography

[1] F. Affentrange and R. Schneider. Random projections of regular simplices. *Discrete and Computational Geometry*, 7(3):219 226, 1992.

[2] R. G. Baraniuk, V. Cevher, M. F. Duarte, and C. Hegde. Model based compressive sensing. *IEEE Trans. on Information Theory*, 56:1982–2001, April 2010.

[3] T. Blumensath and M. E. Davis. Iterative hard thresholding for compressed sensing. arxiv:0805.0510v1, The University of Edinburgh, 2008.

[4] T. Blumensath and M. E. Davis. Sampling theorems for signals from the union of finite-dimensional linear subspaces. *IEEE Transactions on Information Theory*, 55(4), April 2009.

[5] E. Candès and T. Tao. Decoding by linear programming. *IEEE Trans. on Information Theory*, 51(12):4203 4215, December 2005.

[6] D. Donoho. Neighborly polytopes and sparse solutions of underdetermined linear equations. Technical report, Department of Statistics, Stanford University, 2004.

[7] D. Donoho. High dimensional centrally symmetric polytopes with neighborliness proportional to dimension. *Discrete and Computational Geometry*, 102(27):617–652, 2006.

[8] H. Hadwiger. Gitterpunktanzahl im Simplex und Willssche Vermutung. *Math. Ann.*, 239:271–288, 1979.

[9] P. McMullen. Non-linear angle-sum relations for polyhedral cones and polytopes. *Math. Proc. Cambridge Philos. Soc.*, 78(2):247–261, 1975.

[10] D. Needell and J. A. Tropp. CoSaMP: Iterative signal recovery from incomplete and inaccurate samples. *Appl. Comput. Harmon. Anal.*, 26(3):301–321, 2009.

[11] L. A. Santaló. Geometría integral en espacios de curvatura constante. *Rep. Argentina Publ. Com. Nac. Energí Atómica, Ser. Mat 1, No. 1*, 1952.

[12] A.M. Vershik and P. V. Sporyshev. Asymptotic behavior of the number of faces of random polyhedra and the neighborliness problem. *Selecta Mathematica Sovietica*, 11(2):181–201, 1992.

[13] W. Xu. *Compressive Sensing for Sparse Approximations: Construction, Algorithms and Analysis.* PhD thesis, California Institute of Technology, Department of Electrical Engineering, 2010.